

AD-A173 057

DEVELOPMENT OF A THEORETICALLY SOUND CAP MODEL FOR
FITTING ISST-TYPE MATE. (U) ARMY ENGINEER WATERWAYS
EXPERIMENT STATION VICKSBURG MS STRUC.. G Y BALADI

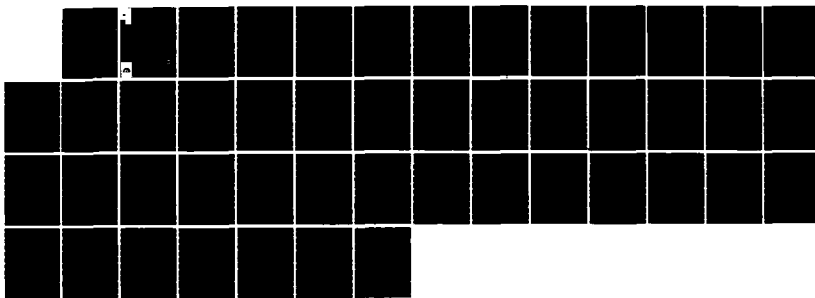
1/1

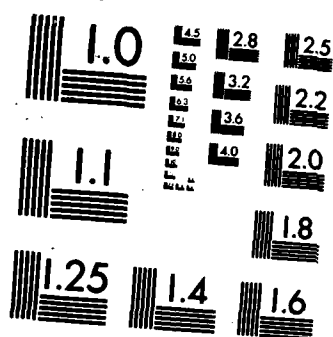
UNCLASSIFIED

OCT 86 WES/TR/SL-86-34

F/G 8/13

NL



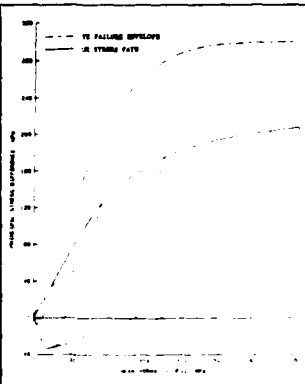
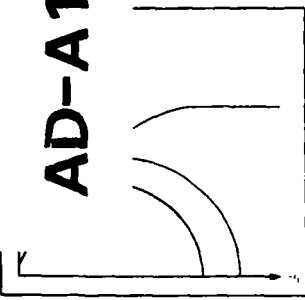


MICROCOPY RESOLUTION TEST CHART
NATIONAL BUREAU OF STANDARDS-1963-A



US Army Corps
of Engineers

AD-A173 057



DTIC FILE COPY



October 1986
Final Report

Approved For Public Release; Distribution Unlimited

DTIC
ELECTED
OCT 16 1986
S D
B

Prepared for Ballistic Missile Office
Norton Air Force Base, California 92409-6468
Under MIPR No. FY 7653-85-04020

411415 SH

86 10 16 134

(2)

**Destroy this report when no longer needed. Do not return
it to the originator.**

**The findings in this report are not to be construed as an official
Department of the Army position unless so designated
by other authorized documents.**

**The contents of this report are not to be used for
advertising, publication, or promotional purposes.
Citation of trade names does not constitute an
official endorsement or approval of the use of
such commercial products.**

Unclassified

SECURITY CLASSIFICATION OF THIS PAGE

REPORT DOCUMENTATION PAGE				Form Approved OMB No 0704-0188 Exp Date Jun 30, 1986									
1a. REPORT SECURITY CLASSIFICATION Unclassified		1b. RESTRICTIVE MARKINGS											
2a. SECURITY CLASSIFICATION AUTHORITY		3. DISTRIBUTION/AVAILABILITY OF REPORT Approved for public release; distribution unlimited.											
2b. DECLASSIFICATION/DOWNGRADING SCHEDULE													
4. PERFORMING ORGANIZATION REPORT NUMBER(S) Technical Report SL-86-34		5. MONITORING ORGANIZATION REPORT NUMBER(S)											
6a. NAME OF PERFORMING ORGANIZATION USAEWES Structures Laboratory		6b. OFFICE SYMBOL (If applicable) WESSD	7a. NAME OF MONITORING ORGANIZATION										
6c. ADDRESS (City, State, and ZIP Code) PO Box 631 Vicksburg, MS 39180-0631		7b. ADDRESS (City, State, and ZIP Code)											
8a. NAME OF FUNDING/SPONSORING ORGANIZATION Ballistic Missile Office		8b. OFFICE SYMBOL (If applicable)	9. PROCUREMENT INSTRUMENT IDENTIFICATION NUMBER										
8c. ADDRESS (City, State, and ZIP Code) Norton Air Force Base, CA 92409-6468		10. SOURCE OF FUNDING NUMBERS See reverse PROGRAM ELEMENT NO. PROJECT NO. TASK NO. WORK UNIT ACCESSION NO.											
11. TITLE (Include Security Classification) Development of a Theoretically Sound Cap Model for Fitting ISST-Type Material Behavior													
12. PERSONAL AUTHOR(S) Baladi, George Y.													
13a. TYPE OF REPORT Final report	13b. TIME COVERED FROM _____ TO _____		14. DATE OF REPORT (Year, Month, Day) October 1986	15. PAGE COUNT 46									
16. SUPPLEMENTARY NOTATION This report was originally published as a draft report to the sponsor in November 1985.													
17. COSATI CODES <table border="1"><tr><th>FIELD</th><th>GROUP</th><th>SUB-GROUP</th></tr><tr><td> </td><td> </td><td> </td></tr><tr><td> </td><td> </td><td> </td></tr></table>		FIELD	GROUP	SUB-GROUP							18. SUBJECT TERMS (Continue on reverse if necessary and identify by block number) See reverse		
FIELD	GROUP	SUB-GROUP											
19. ABSTRACT (Continue on reverse if necessary and identify by block number) - This report describes the development of a three-dimensional elastic-plastic work-hardening constitutive relationship in which the shear modulus is a function of plastic volumetric strain and the second invariant of the strain deviation tensor. It contains (1) the general description of the new model including the proof of its theoretical soundness, (2) selected mathematical forms of its various response functions, and (3) an example model fit to the material properties specified for ISST Layer 2.													
20. DISTRIBUTION/AVAILABILITY OF ABSTRACT <input checked="" type="checkbox"/> UNCLASSIFIED/UNLIMITED <input type="checkbox"/> SAME AS RPT <input type="checkbox"/> DTIC USERS		21. ABSTRACT SECURITY CLASSIFICATION Unclassified											
22a. NAME OF RESPONSIBLE INDIVIDUAL		22b. TELEPHONE (Include Area Code)	22c. OFFICE SYMBOL										

10. SOURCE OF FUNDING NUMBERS (Continued).

MIPR No. FY 7653-85-04020, dated 24 January 1985.

18. SUBJECT TERMS (Continued).

Complementary strain energy function	Elastic-plastic behavior
Constitutive models	ISST soil properties
Elastic media	Stress-strain relations
	Tension cutoff criteria

PREFACE

The study reported herein was conducted by personnel of the US Army Engineer Waterways Experiment Station (WES), Geomechanics Division (GD), Structures Laboratory (SL). The work was funded by the Air Force Ballistic Missile Office under FY 85 MIPR No. FY 7653-85-04020, dated 24 January 1985.

The study was conducted by Dr. George Y. Baladi, GD, under the general direction of Dr. J. G. Jackson, Jr., Chief, GD. The report was written by Dr. Baladi, reviewed by Dr. Jackson, typed by Mrs. P. A. Sullivan, and was transmitted to the sponsor in November 1985.

COL Allen F. Grum, USA, was the previous Director of WES. COL Dwayne G. Lee, CE, is the present Commander and Director. Dr. Robert W. Whalin is Technical Director. Mr. Bryant Mather is Chief, SL.

Accession No.	
NTIS GRUM	
DTIC TR	
Unclassified	
Justification	
By _____	
Distribution	
Availability Codes	
Dist	Final and/or Original
A-1	



CONTENTS

	<u>Page</u>
PREFACE	i
LIST OF ILLUSTRATIONS	iii
CONVERSION FACTORS, NON-SI TO SI (METRIC) UNITS OF MEASUREMENT	v
INTRODUCTION	1
GENERAL DESCRIPTION OF THE NEW MODEL	1
Elastic Strain Increment Tensor	4
Plastic Strain Increment Tensor	7
Total Strain Increment Tensor	9
Behavior in Tension	10
EXAMPLE MODEL FIT FOR ISST LAYER 2	11
Yield Conditions	11
Hardening Function	12
Bulk Modulus	12
Shear Modulus	13
Numerical Values of Fitting Parameters	14
ACKNOWLEDGEMENT	14
REFERENCES	37

LIST OF ILLUSTRATIONS

<u>Figure</u>		<u>Page</u>
1	Uniaxial strain (UX) stress paths for ISST materials	16
2	Typical yield surfaces for an elastic-plastic work hardening cap model	17
3	Behavior of the model in tension	18
4	Material properties for ISST Layer 2: uniaxial strain compressibility relation to $\sigma_z = 150$ MPa	19
5	Material properties for ISST Layer 2: uniaxial strain compressibility relation to $\sigma_z = 800$ MPa	20
6	Material properties for ISST Layer 2: UX stress path to $\sigma_z = 75$ MPa and TX failure envelope	21
7	Material properties for ISST Layer 2: UX stress path to $\sigma_z = 800$ MPa and TX failure envelope	22
8	Material properties for ISST Layer 2: triaxial compression stress-strain relations for low confining pressures	23
9	Material properties for ISST Layer 2: triaxial compression stress-strain relations for intermediate confining pressures ..	24
10	Material properties for ISST Layer 2: triaxial compression stress-strain relations for high confining pressures	25
11	Strain-dependent cap model fit for ISST Layer 2: uniaxial strain compressibility relation to $\sigma_z = 155$ MPa	26
12	Strain-dependent cap model fit for ISST Layer 2: uniaxial strain compressibility relation to $\sigma_z = 470$ MPa	27
13	Strain-dependent cap model fit for ISST Layer 2: uniaxial strain compressibility relation to $\sigma_z = 860$ MPa	28
14	Strain-dependent cap model fit for ISST Layer 2: uniaxial strain compressibility relation to $\sigma_z = 2,000$ MPa	29
15	Strain-dependent cap model fit for ISST Layer 2: UX stress path to $\sigma_z = 80$ MPa and TX failure envelope	30
16	Strain-dependent cap model fit for ISST Layer 2: UX stress path to $\sigma_z = 860$ MPa and TX failure	31
17	Strain-dependent cap model fit for ISST Layer 2: UX stress path to $\sigma_z = 2,500$ MPa and TX failure envelope	32
18	Strain-dependent cap model fit for ISST Layer 2: triaxial compression stress-strain relations for low confining pressures	33
19	Strain-dependent cap model fit for ISST Layer 2: triaxial compression stress-strain relations for high confining pressures	34

LIST OF ILLUSTRATIONS (Continued)

<u>Figure</u>		<u>Page</u>
20	Strain-dependent cap model fit for ISST Layer 2: triaxial compression principal stress difference - vertical strain relations for low confining pressures	35
21	Strain-dependent cap model fit for ISST Layer 2: triaxial compression principal stress difference - vertical strain relations for high confining pressures	36

**CONVERSION FACTORS, NON-SI TO SI (METRIC)
UNITS OF MEASUREMENT**

Non-SI units of measurement used in this report can be converted to SI (metric) units as follows:

Multiply	By	To Obtain
degrees (angle)	0.01745329	radians
feet	0.3048	meters
gallons (US liquid)	3.785412	cubic decimeters (litres)
inches	2.54	centimeters
kips (force)	4.448222	kilonewtons
kips (force) per square inch	6.894757	megapascals
megatons (nuclear equivalent of TNT)	4.184	petajoules
pounds (force) per square inch	6.894757	kilopascals
pounds (mass)	0.4535924	kilograms
pounds (mass) per cubic foot	16.01846	kilograms per cubic meter

DEVELOPMENT OF A THEORETICALLY SOUND CAP MODEL
FOR FITTING ISST-TYPE MATERIAL BEHAVIOR

INTRODUCTION

Incremental elastic-plastic constitutive models which include both an ultimate failure envelope and a work-hardening yield surface -- or cap -- are commonly used in ground shock calculations to simulate geologic material behavior (Reference 1). The elastic shear modulus in the cap model is usually formulated in terms of the second invariant of the stress deviation tensor J_2^e and the plastic volumetric strain ϵ_{kk}^P . Such formulations, however, cannot replicate the highly nonlinear bowl-shaped unloading stress paths that typify ISST-type material behavior (Reference 2 and Figure 1).

In 1984, a cap model was developed in which the shear modulus was formulated not only as a function of J_2^e and ϵ_{kk}^P , but also as function of the third invariant of the stress deviation tensor J_3^e (Reference 3). Although this model fit the recommended ISST material properties quite well, it did not satisfy all of the vigorous theoretical constraints outlined by Dr. Ivan S. Sandler of Weidlinger Associates as a prerequisite for use of a constitutive model in explosive-induced ground shock and soil/structure interaction codes (Reference 4). In order to satisfy these theoretical requirements and still satisfactorily replicate ISST-type material behavior, a new cap model has been formulated in which the shear modulus is expressed as a function of ϵ_{kk}^P and the second invariant of the strain deviation tensor I_2^e . In addition to its theoretical soundness, the model has the advantage for finite element calculations of not requiring any additional storage since I_2^e can be calculated directly from displacements. Strain-dependent models also have an advantage over stress-dependent models in that they can be numerically incorporated into computer codes so as to be insensitive to increment size.

A general description of the strain-dependent cap model and the associated theoretical proofs follows.

GENERAL DESCRIPTION OF THE NEW MODEL

The basic premise of elastic-plastic constitutive models is the assumption that certain materials are capable of undergoing small plastic (permanent) as well as elastic (recoverable) strains at each loading increment.

Mathematically, the total strain increment is assumed to be the sum of the elastic and plastic strain increments; i.e.,

$$d\epsilon_{ij} = d\epsilon_{ij}^E + d\epsilon_{ij}^P \quad (1)$$

where

$d\epsilon_{ij}$ = components of the total strain increment tensor

$d\epsilon_{ij}^E$ = components of the elastic strain increment tensor

$d\epsilon_{ij}^P$ = components of the plastic strain increment tensor

Within the elastic range, the behavior of the material can be described by an elastic constitutive relation of the type

$$d\epsilon_{ij}^E = C_{ijkl}(\sigma_{mn}) d\sigma_{kl} \quad (2)$$

where

C_{ijkl} = material response function

$d\sigma_{kl}$ = components of stress increment tensor

The behavior of the material in the plastic range can be described within the framework of the generalized incremental theory of plasticity. The mathematical basis of the theory was established by Drucker (Reference 5), who introduced the concept of material stability; this concept has the following implications:

1. The yield surface (loading function) should be convex in stress space.
2. The yield surface and the plastic potential should coincide (which results in an "associated" flow rule).
3. Work "softening" should not occur.

These three conditions can be summarized mathematically by the following inequality

$$d\sigma_{ij} d\epsilon_{ij}^P \geq 0 \quad (3)$$

These conditions allow considerable flexibility in the choice of the form of the loading function f for the model, which serves as both a yield surface and the plastic potential. In general, the yield surface may be expressed as

$$f(\sigma_{ij}, \kappa) = 0 \quad (4)$$

and for isotropic materials the yield surface may be expressed, for example, as

$$f(J_1, \sqrt{J_2}, \kappa) = 0 \quad (5)$$

where

$J_1 = \sigma_{nn}$ = first invariant of the stress tensor

$J_2 = \frac{1}{2} S_{ij} S_{ij}$ = second invariant of the stress deviation tensor

$S_{ij} = \sigma_{ij} - (J_1/3) \delta_{ij}$ = stress deviation tensor

δ_{ij} = Kronecker delta = $\begin{cases} 1 & i = j \\ 0 & i \neq j \end{cases}$

κ = a hardening parameter

The hardening parameter κ can generally be taken to be a function of the plastic strain tensor ϵ_{ij}^P . The yield surface of Equation 4 or 5 may expand or contract as κ increases or decreases, respectively (Figure 2).

Conditions 1 through 3 above, taken in conjunction with Equation 4 or 5, result in the following plastic flow rule for isotropic materials:

$$d\epsilon_{ij}^P = \begin{cases} d\lambda \frac{\partial f}{\partial \sigma_{ij}} & \text{if } f = 0 \\ 0 & \text{if } f < 0 \end{cases} \quad (6)$$

where $d\lambda$ is a positive scalar factor of proportionality, which is non-zero only when plastic deformations occur and is dependent on the particular form of the loading function.

Elastic Strain Increment Tensor

For isotropic elastic materials, the strain increment tensor (Equation 2) takes the following form

$$d\epsilon_{ij}^E = \frac{dJ_1}{9K} \delta_{ij} + \frac{1}{2G} dS_{ij} \quad (7)$$

or

$$d\sigma_{ij} = K d\epsilon_{kk}^E \delta_{ij} + 2G d\epsilon_{ij}$$

where K is the elastic bulk modulus and G is the elastic shear modulus. These moduli can be functions of the invariants of either the stress or the strain tensor. Accordingly, it is assumed that $K = K(J_1, J_2^I, J_3^I)$ and $G = G(J_1, J_2^I, J_3^I)$ or $K = K(I_1, I_2^I, I_3^I)$ and $G = G(I_1, I_2^I, I_3^I)$. Equation 7 can be written in terms of the hydrostatic and deviatoric components of the strain and stress increment tensors; i.e.,

$$\begin{aligned} d\epsilon_{kk}^E &= \frac{1}{3K(J_1, J_2^I, J_3^I)} dJ_1 \\ d\epsilon_{ij}^E &= \frac{1}{2G(J_1, J_2^I, J_3^I)} dS_{ij} \end{aligned} \quad (8)$$

or

$$\begin{aligned} dJ_1 &= 3K(I_1, I_2^I, I_3^I) d\epsilon_{kk}^E \\ dS_{ij} &= 2G(I_1, I_2^I, I_3^I) d\epsilon_{ij}^E \end{aligned} \quad (9)$$

where

$d\epsilon_{kk}^E$ = increment of elastic volumetric strain

$d\epsilon_{ij}^E$ = elastic strain deviation increment tensor

$J_3^I = \frac{1}{3} S_{ij} S_{jk} S_{ki}$ = third invariant of the stress deviation tensor

$I_1 = \epsilon_{kk}$ = first invariant of the strain tensor

$I_2^I = \frac{1}{2} e_{ij} e_{ij}$ = second invariant of the strain deviation tensor

$I_3^I = \frac{1}{3} e_{ij} e_{jk} e_{ki}$ = third invariant of the strain deviation tensor

In order not to generate energy or hysteresis within the elastic range, the elastic behavior of the model must be path independent. The material should then possess a positive definite elastic internal energy function \bar{W} which is independent of stress path. The strain energy function can be written as

$$\begin{aligned}
 \bar{W} &= \int_0^{\epsilon_{ij}} \sigma_{ij} d\epsilon_{ij}^E \\
 &= \int_0^{\sigma_{ij}} (S_{ij} + \frac{1}{3} J_1 \delta_{ij}) \left[\frac{J_1}{9K(J_1, J_2, J_3)} \delta_{ij} + \frac{dS_{ij}}{2G(J_1, J_2, J_3)} \right] \\
 &= \int_0^{J_1} \frac{J_1}{9K(J_1, J_2, J_3)} dJ_1 + \int_0^{S_{ij}} \frac{1}{2G(J_1, J_2, J_3)} S_{ij} dS_{ij} \\
 &= \int_0^{J_1} \frac{d(J_1)^2}{18K(J_1, J_2, J_3)} + \int_0^{J_2} \frac{dJ_2}{2G(J_1, J_2, J_3)} \quad (10)
 \end{aligned}$$

In order for \bar{W} to be independent of stress path, the integrals in Equation 10 have to depend only on the current values of J_1 and J_2 . Therefore, the bulk and shear moduli have to be expressed as

$$\begin{aligned}
 K &= K(J_1) \\
 G &= G(J_2) \quad (11)
 \end{aligned}$$

Similarly, the complementary strain energy function W^D can be written as

$$\begin{aligned}
 W^D &= \int_0^{\sigma_{ij}} \epsilon_{ij} d\sigma_{ij} \\
 &= \int_0^{\epsilon_{ij}} \left(\frac{\epsilon_{kk}}{3} \delta_{ij} + e_{ij} \right) \left[K(I_1, I_2, I_3) d\epsilon_{kk}^E \delta_{ij} + 2G(I_1, I_2, I_3) de_{ij}^E \right] \quad (12)
 \end{aligned}$$

Substitution of Equation 1 into Equation 12 leads to

$$W^D = \int_0^{\epsilon_{ij}} \left(\frac{\epsilon_{kk}}{3} \delta_{ij} + e_{ij} \right) [K(I_1, I_2, I_3)(de_{kk} - de_{kk}^P) \delta_{ij} + 2G(I_1, I_2, I_3)(de_{ij} - de_{ij}^P)] \quad (13)$$

But de_{kk}^P and de_{ij}^P equal to zero under elastic deformation. Hence Equation 13 becomes

$$\begin{aligned} W^D &= \int_0^{\epsilon_{ij}} \left(\frac{\epsilon_{kk}}{3} \delta_{ij} + e_{ij} \right) [K(I_1, I_2, I_3)de_{kk} \delta_{ij} + 2G(I_1, I_2, I_3)de_{ij}] \\ &= \int_0^{\epsilon_{kk}} \frac{1}{2} K(I_1, I_2, I_3) d[\epsilon_{kk}^2] + \int_0^{I_2} 2G(I_1, I_2, I_3) dI_2 \end{aligned} \quad (14)$$

Equation 14 indicates that for W^D to be independent of the strain path, the integrals in Equation 14 have to depend only on the current values of I_1 and I_2 . Therefore, the bulk and shear moduli can also be expressed as

$$K = K(\epsilon_{kk}) = K(I_1) \quad (15)$$

$$G = G(I_2)$$

It can be concluded from Equations 11 and 15 that the bulk modulus should be expressed as a function of either I_1 or J_1 , and the shear modulus should be related to either I_2 or J_2 . Further, K and G must always be positive. Since during elastic deformation the hardening parameter κ is constant, the bulk and shear moduli can also be expressed as

$$\begin{aligned} K &= K(J_1, \kappa) = K(I_1, \kappa) \\ G &= G(J_2, \kappa) = G(I_2, \kappa) \end{aligned} \quad (16)$$

Plastic Strain Increment Tensor

The plastic strain increment tensor is given by Equation 6 where the loading function f is given by Equation 4 or 5. The hardening parameter in Equation 4 or 5 could be taken as being equal to the plastic volumetric strain ϵ_{kk}^P ; thus

$$\kappa = \epsilon_{kk}^P \quad (17)$$

The use of Equation 17 will allow the cap to expand as well as to contract (Figure 2). The plastic loading criteria for the function f are given as

$$\frac{\partial f}{\partial \sigma_{ij}} d\sigma_{ij} \left\{ \begin{array}{l} > 0 \text{ for loading} \\ = 0 \text{ for neutral loading} \\ < 0 \text{ for unloading} \end{array} \right. \quad (18)$$

Because $d\epsilon_{ij}^P = 0$ during unloading or neutral loading, as well as for $f < 0$, Equations 7 and/or 8 and 9 are used to determine the purely elastic strain changes. The prescription that neutral loading produces no plastic strain is called the continuity condition. Its satisfaction leads to coincidence of the elastic and plastic constitutive laws during neutral loading.

Like the elastic behavior, the plastic stress-strain relation can be expressed in terms of the hydrostatic and deviatoric components of strain. Applying the chain rule of differentiation to the right-hand side of Equation 6 yields

$$\text{or } d\epsilon_{ij}^P = d\lambda \left(\frac{\partial f}{\partial J_1} \frac{\partial J_1}{\partial \sigma_{ij}} + \frac{\partial f}{\partial \sqrt{J_2}} \frac{\partial \sqrt{J_2}}{\partial \sigma_{ij}} \right) \quad (19)$$

$$d\epsilon_{ij}^P = d\lambda \left(\frac{\partial f}{\partial J_1} \delta_{ij} + \frac{1}{2\sqrt{J_2}} \frac{\partial f}{\partial \sqrt{J_2}} S_{ij} \right)$$

Multiplying both sides of Equation 19 by δ_{ij} gives

$$d\epsilon_{kk}^P = 3 d\lambda \frac{\partial f}{\partial J_1} \quad (20)$$

The deviatoric component of the plastic strain increment tensor $d\epsilon_{ij}^P$ can be written as

$$d\epsilon_{ij}^P = d\epsilon_{ij}^P - \frac{1}{3} d\epsilon_{kk}^P \delta_{ij} \quad (21)$$

Substitution of Equations 19 and 20 into Equation 21 yields

$$d\epsilon_{ij}^P = \frac{d\lambda}{2\sqrt{J_2}} \frac{\partial f}{\partial \sqrt{J_2}} S_{ij} \quad (22)$$

In order to use Equation 19 or Equations 20 and 22, the proportionality factor $d\lambda$ must be determined. This can be accomplished in the following manner. From Equations 5 and 17 the total derivative of f becomes

$$df = \frac{\partial f}{\partial J_1} dJ_1 + \frac{1}{2\sqrt{J_2}} \frac{\partial f}{\partial \sqrt{J_2}} S_{ij} dS_{ij} + \frac{\partial f}{\partial \epsilon_{kk}^P} d\epsilon_{kk}^P = 0 \quad (23)$$

In view of Equations 8 or 9 and 20, Equation 23 becomes

$$3K d\epsilon_{kk}^E \frac{\partial f}{\partial J_1} + \frac{G d\epsilon_{ij}^E}{\sqrt{J_2}} \frac{\partial f}{\partial \sqrt{J_2}} S_{ij} + 3 d\lambda \frac{\partial f}{\partial J_1} \frac{\partial f}{\partial \epsilon_{kk}^P} = 0 \quad (24)$$

Substituting Equation 1 into Equation 24 results in

$$3K(d\epsilon_{kk} - d\epsilon_{kk}^P) \frac{\partial f}{\partial J_1} + \frac{G}{\sqrt{J_2}} (d\epsilon_{ij} - d\epsilon_{ij}^P) \frac{\partial f}{\partial \sqrt{J_2}} S_{ij} = -3 d\lambda \frac{\partial f}{\partial J_1} \frac{\partial f}{\partial \epsilon_{kk}^P} \quad (25)$$

or

$$3K \frac{d\epsilon_{kk}}{\partial J_1} \frac{\partial f}{\partial J_1} + \frac{G}{\sqrt{J_2}} \frac{\partial f}{\partial \sqrt{J_2}} S_{ij} d\epsilon_{ij} = 3K \frac{d\epsilon_{kk}^P}{\partial J_1} \frac{\partial f}{\partial J_1} + \frac{G}{\sqrt{J_2}} \frac{\partial f}{\partial \sqrt{J_2}} S_{ij} d\epsilon_{ij}^P - 3 d\lambda \frac{\partial f}{\partial J_1} \frac{\partial f}{\partial \epsilon_{kk}^P} \quad (26)$$

Substituting the values of $d\epsilon_{kk}^P$ and $d\epsilon_{ij}^P$ from Equations 20 and 22, respectively, into Equation 26 yields

$$3K \frac{d\epsilon_{kk}}{\partial J_1} \frac{\partial f}{\partial J_1} + \frac{G}{\sqrt{J_2}} \frac{\partial f}{\partial \sqrt{J_2}} S_{ij} d\epsilon_{ij} = 9K d\lambda \left(\frac{\partial f}{\partial J_1} \right)^2 + G d\lambda \left(\frac{\partial f}{\partial \sqrt{J_2}} \right)^2 - 3 d\lambda \frac{\partial f}{\partial J_1} \frac{\partial f}{\partial \epsilon_{kk}^P} \quad (27)$$

Solving for $d\lambda$ gives

$$d\lambda = \frac{3K \frac{\partial f}{\partial J_1} d\epsilon_{kk} + \frac{G}{\sqrt{J_2}} \frac{\partial f}{\partial \sqrt{J_2}} S_{ij} d\epsilon_{ij}}{9K \left(\frac{\partial f}{\partial J_1} \right)^2 + G \left(\frac{\partial f}{\partial \sqrt{J_2}} \right)^2 - 3 \frac{\partial f}{\partial J_1} \frac{\partial f}{\partial \epsilon_{kk}^P}} \quad (28)$$

Total Strain Increment Tensor

The total strain increment tensor can be obtained by combining Equations 1, 7, 19, and 28:

$$d\epsilon_{ij} = \frac{dJ_1}{9K} \delta_{ij} + \frac{ds_{ij}}{2G}$$

$$+ \left[\frac{3K \frac{\partial f}{\partial J_1} d\epsilon_{kk} + \frac{G}{\sqrt{J_2}} \frac{\partial f}{\partial \sqrt{J_2}} S_{mn} de_{mn}}{9K \left(\frac{\partial f}{\partial J_1} \right)^2 + G \left(\frac{\partial f}{\partial \sqrt{J_2}} \right)^2 - 3 \frac{\partial f}{\partial J_1} \frac{\partial f}{\partial \epsilon_{kk}^P}} \right] \left(\frac{\partial f}{\partial J_1} \delta_{ij} + \frac{1}{2\sqrt{J_2}} \frac{\partial f}{\partial \sqrt{J_2}} S_{ij} \right) \quad (29)$$

Similarly, the stress increment tensor can be written as

$$d\sigma_{ij} = K d\epsilon_{kk} \delta_{ij} + 2G de_{ij}$$

$$- \left[\frac{3K \frac{\partial f}{\partial J_1} d\epsilon_{kk} + \frac{G}{\sqrt{J_2}} \frac{\partial f}{\partial \sqrt{J_2}} S_{mn} de_{mn}}{9K \left(\frac{\partial f}{\partial J_1} \right)^2 + G \left(\frac{\partial f}{\partial \sqrt{J_2}} \right)^2 - 3 \frac{\partial f}{\partial J_1} \frac{\partial f}{\partial \epsilon_{kk}^P}} \right] \left(3K \frac{\partial f}{\partial J_1} \delta_{ij} + G \frac{\partial f}{\partial \sqrt{J_2}} \frac{S_{ij}}{\sqrt{J_2}} \right) \quad (30)$$

Equation 29 or Equation 30 is the general constitutive equation for an elastic-plastic isotropic material. To use either of these equations it is necessary only to specify the functional forms of K , G , and f and, of course, to determine experimentally the numerical values of the coefficients in these functions.

Behavior in Tension

The tension cutoff is triggered in this model whenever the following relation is satisfied:

$$\frac{J_1}{3} - T \geq 0 \quad (31)$$

in which T is the maximum value that the mean hydrostatic tension $\frac{J_1}{3}$ can attain. The volumetric strain which occurs during tension is computed from the following relation:

$$\epsilon_{kk}^T = \frac{\left(\frac{J_1}{3} - T \right)^{\text{POS}}}{K_1} \quad (32)$$

where K_1 is the bulk modulus of the material at $\frac{J_1}{3} = T$ (Figure 3).

Upon reloading, the material stays in the state of tension until the volumetric strain computed by Equation 32 is completely recovered.

EXAMPLE MODEL FIT FOR ISST LAYER 2

To illustrate the new model's capability for fitting ISST-type material behavior, selected mathematical forms of the various response functions were used to fit the material properties for ISST Layer 2 shown in Figures 4 through 10. In the following model response functions, tension is considered positive.

Yield Conditions

The yield conditions consist of an ultimate failure surface of the form

$$f = F(J_1, \sqrt{J_2}) = \sqrt{J_2} - [A - C \exp(BJ_1 - B_1 J_1^2)] = 0 \quad (33)$$

and a work-hardening cap of the form

$$f = H(J_1, \sqrt{J_2}, \epsilon_{kk}^P) = (J_1 - L)^2 + R J_2^2 - (X - L)^2 = 0 \quad (34)$$

where

J_1 = first invariant of the stress tensor

J_2 = second invariant of the stress deviation tensor

A, B, B₁, and C = material parameters (constants)

ϵ_{kk}^P = plastic volumetric strain

$L(\epsilon_{kk}^P)$ and $X(\epsilon_{kk}^P)$ = respectively, the values of J_1 at the center of the cap (Equation 34) and the intersection of the cap with the J_1 axis, and are related as:

$$L - X = R[A - C \exp(BL - B_1 L^2)] \quad (35)$$

where R is the ratio of the major to the minor axis of the cap and is given by:

$$R = \frac{R_0}{1-R_1} [1-R_1 \exp(R_2 L)] + R_3 \left[\frac{R_4-1}{R_4+1} + \frac{1-R_4 \exp(R_5 L)}{1+R_4 \exp(R_5 L)} \right] \quad (36)$$

where R_0 , R_1 , R_2 , R_3 , R_4 , and R_5 are material parameters (constants), and

$$L(\epsilon_{kk}^P) = \begin{cases} l(\epsilon_{kk}^P) & \text{if } l(\epsilon_{kk}^P) \leq 0 \\ 0 & \text{if } l(\epsilon_{kk}^P) > 0 \end{cases} \quad (37)$$

Hardening Function

The hardening function is chosen to be

$$\epsilon_{kk}^P = W[\exp(D_{LL}) - 1 - D_{LL}\exp(D_{1LL})] - D_2 LL^2 \cdot \exp(D_3 LL) \quad (38)$$

in which

$$\overline{LL} = L - \overline{ll} \quad (39)$$

where

W , D , D_1 , D_2 , and D_3 = material constants.

W in Equation 38 defines the maximum plastic volumetric compaction that the material can experience under hydrostatic loading. The numerical value of \overline{ll} is the solution of the following equation

$$\overline{ll} - R[A - C\exp(B\overline{ll} - B_1\overline{ll}^2)] = 0 \quad (40)$$

Bulk Modulus

The bulk modulus was taken to be a function of the plastic volumetric strain and the first invariant of the stress tensor

$$K(J_1, \epsilon_{kk}^P) = \left\{ \frac{K_1}{1-K_1} (1 - K_1 \exp(K_2 \epsilon_{kk}^P)) + K_3 \left[1 + \frac{1 - K_4 \exp(K_5 \epsilon_{kk}^P)}{1 + K_4 \exp(K_5 \epsilon_{kk}^P)} \right] \right\} \times \frac{1}{K_6 M} \left(1 - K_6 M \left[\frac{1 - K_7 \exp(K_8 DSJ_1)}{1 + K_7 \exp(K_8 DSJ_1)} \right] \right) \quad (41)$$

in which

$$K_6 M = \frac{K_6 \cdot R_{KL}}{R_{KJ}} \quad (42)$$

$$K67 = 1 - \frac{K6M(1-K7)}{1+K7} \quad (43)$$

$$RKJL = \min(J1, RKJ) \quad (44)$$

$$DSJ1 = \max \left[\frac{RKJL - J1}{RKJL}, 0 \right] \quad (45)$$

where KI , $K1$, $K2$, $K3$, $K4$, $K5$, $K6$, $K7$, $K8$, and RKJ are material parameters (constants).

Shear Modulus

The shear modulus was taken to be a function of the plastic volumetric strain and the second invariant of the strain deviation tensor:

$$G(\sqrt{I_2^P}, \bar{\epsilon}_{kk}^P) = \max \left\{ \left[\frac{GI}{1-G1} (1-G1 \cdot \exp(G2 \cdot \bar{\epsilon}_{kk}^P)) \right. \right. \\ \left. \left. + G3 \left(1 + \frac{1-G4 \cdot \exp(G5 \cdot \bar{\epsilon}_{kk}^P)}{1+G4 \cdot \exp(G5 \cdot \bar{\epsilon}_{kk}^P)} \right) \right] \cdot \exp(-G6 \cdot DI2), G7 \right\} \quad (46)$$

in which

$$DI2 = (SL - \sqrt{I_2^P}) \left\{ \left[-\frac{1}{G9} \ln \frac{-\bar{\epsilon}_{kk}^P}{G8} \right]^{\frac{1}{2}} + 1 \right. \\ \left. - G10(G11 + \bar{\epsilon}_{kk}^P)^2 \cdot \exp[G12(G11 + \bar{\epsilon}_{kk}^P)] \right\} \quad (47)$$

where

GI , $G1$, $G2$, $G3$, $G4$, $G5$, $G6$, $G7$, $G8$, $G9$, $G10$, $G11$ and $G12$ are material parameters (constants). SL and $\bar{\epsilon}_{kk}^P$ in equation 47 are given by

$$SL = \max [SL, \sqrt{I_2^P}] \quad (48)$$

$$\overline{\epsilon\epsilon}_{kk}^P = \begin{cases} \epsilon_{kk}^P & \text{if } -G8 \leq \epsilon_{kk}^P \leq -G13 \\ -G8 & \text{if } -G8 > \epsilon_{kk}^P \\ -G13 & \text{if } -G13 < \epsilon_{kk}^P \end{cases} \quad (49)$$

where G13 is a material parameter and the initial value of SL is zero.

Numerical Values of Fitting Parameters

The above model includes a total of 39 fitting parameters (or material constants); the numerical values of these parameters used to fit the material properties specified for ISST Layer 2 are given in Table 1. Figures 11-21 depict the stress-strain and strength behavior predicted by the model; the plot scales permit direct comparison with the material property plots given in Figures 4-10.

ACKNOWLEDGEMENT

The author is deeply grateful to Dr. Ivan S. Sandler of Weidlinger Associates for his review of the model and confirmation that it is theoretically sound (Reference 6).

Table 1. Numerical values of fitting parameters for ISST Layer 2.

Model Fitting Parameters		Numerical Value
Name	Notation, Unit	
Bulk Density	ρ , g/cm ³	1.90
Failure Envelope Parameters		
	A, MPa	173.2051
	B, (MPa) ⁻¹	0.0013
	B1, (MPa) ⁻²	12 x 10 ⁻⁷
	C, MPa	172.9164
Hardening Yield Surface Parameters		
	R0, --	2.5
	R1, --	0.0
	R2, (MPa) ⁻¹	0.0
	R3, --	2000.0
	R4, --	1.5 x 10 ⁷
	R5, (MPa) ⁻¹	0.02
	W, --	0.22
	D, (MPa) ⁻¹	0.0105
	D1, (MPa) ⁻¹	0.045
	D2, (MPa) ⁻²	0.00015
	D3, (MPa) ⁻¹	0.04
Bulk Modulus Parameters		
	K1, MPa	2000.0
	K2, --	0.9
	K3, MPa	2.0
	K4, --	10 ⁵
	K5, --	2000.0
	K6, --	24.3
	K7, --	0.8
	K8, --	10 ⁵
	RKJ, MPa	15.0
		-1500.00
Shear Modulus Parameters		
	G1, MPa	1500.0
	G2, --	0.9
	G3, MPa	2.0
	G4, --	0.75 x 10 ⁵
	G5, --	2000.0
	G6, --	22.5
	G7, --	220.0
	G8, --	400.0
	G9, --	0.219829
	G10, --	0.063
	G11, --	12000.0
	G12, --	0.163
	G13, --	120.0
		0.185

PRELIMINARY MATERIAL PROPERTIES FOR ISST: BEST ESTIMATE HIGH-PRESSURE DYNAMIC UX STRESS PATH RESPONSES AND STRENGTH ENVELOPES FOR MILLISECOND-TYPE LOADINGS ON CEMENTED SAND LAYERS 1-3

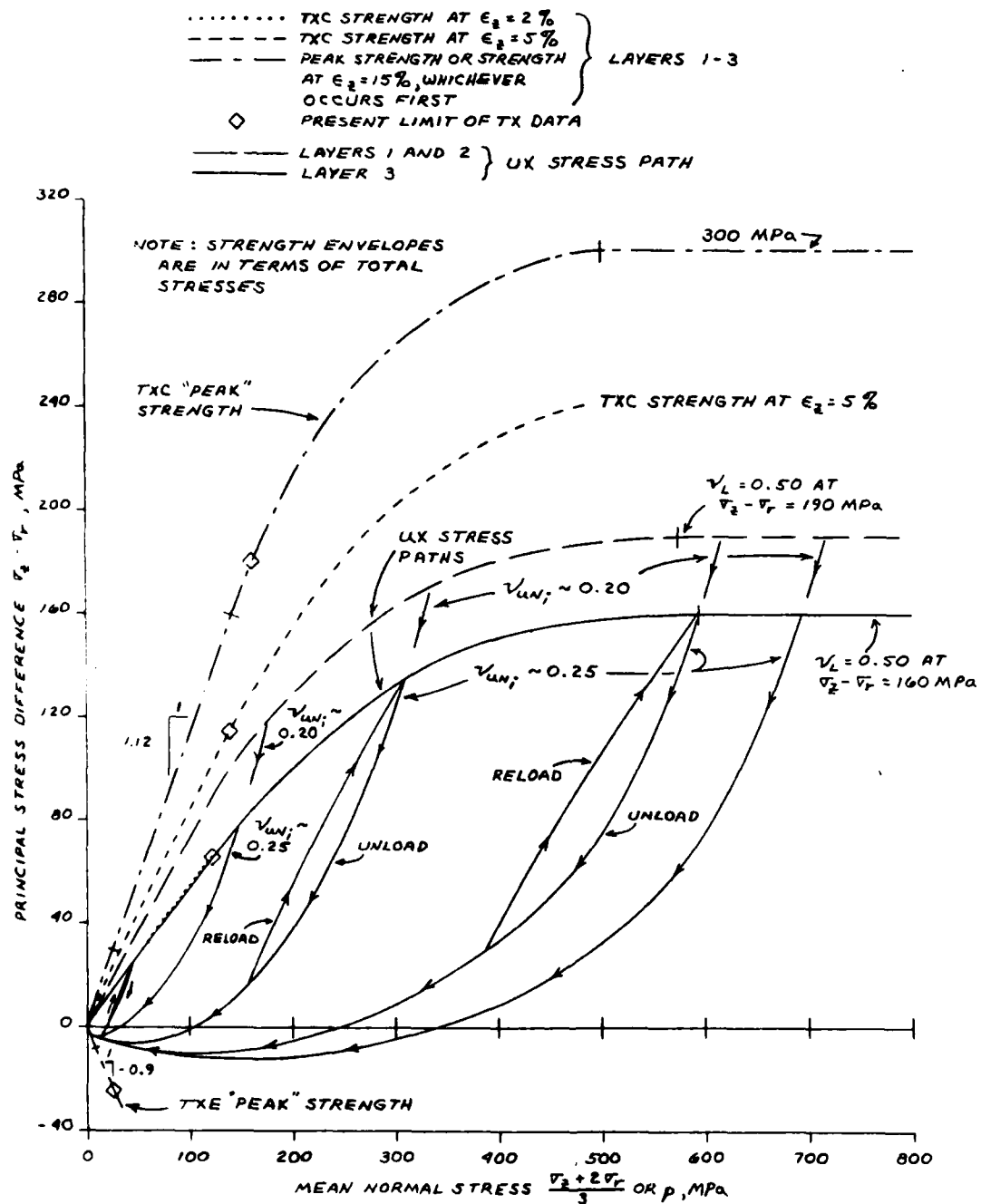


Figure 1. Uniaxial strain (UX) stress paths for ISST materials (extract from Reference 2).

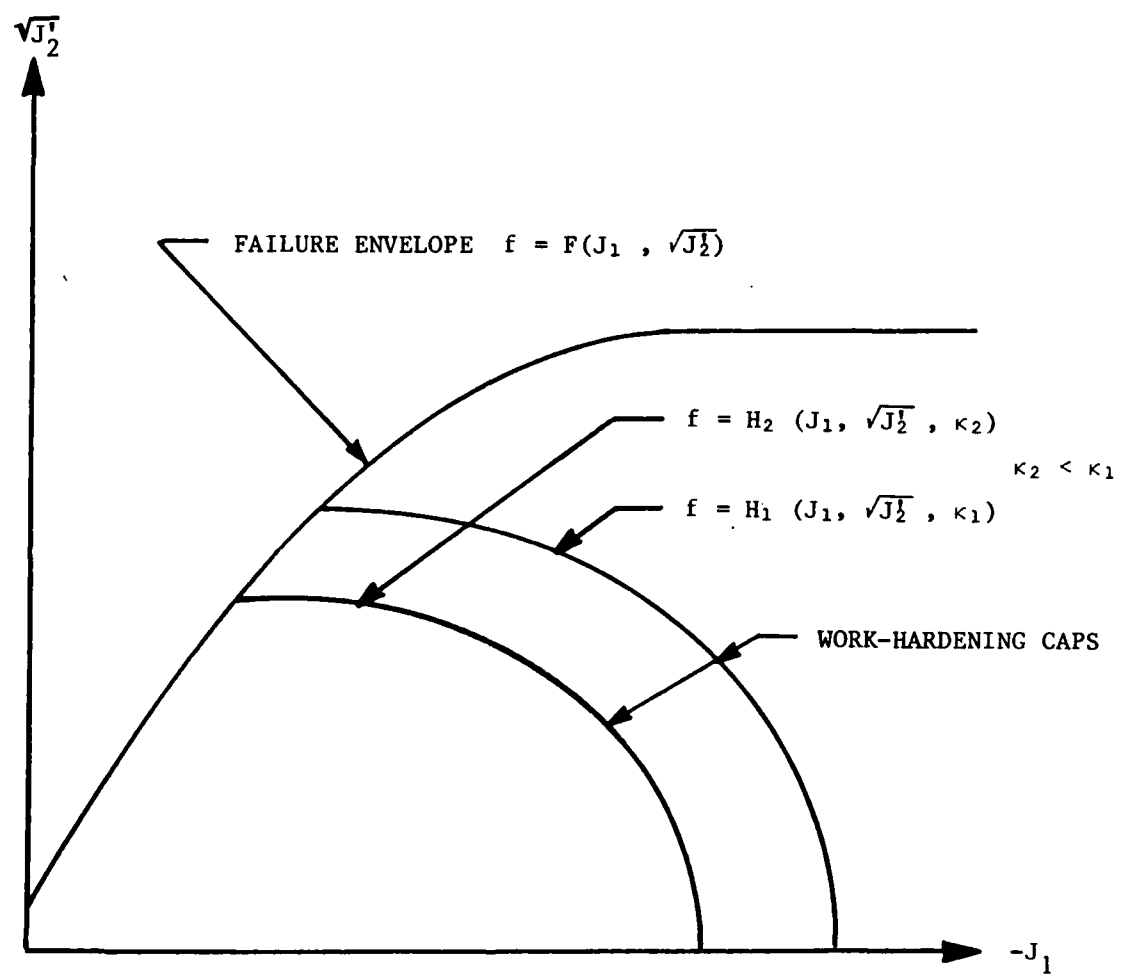


Figure 2. Typical yield surfaces for an elastic-plastic work hardening cap model.

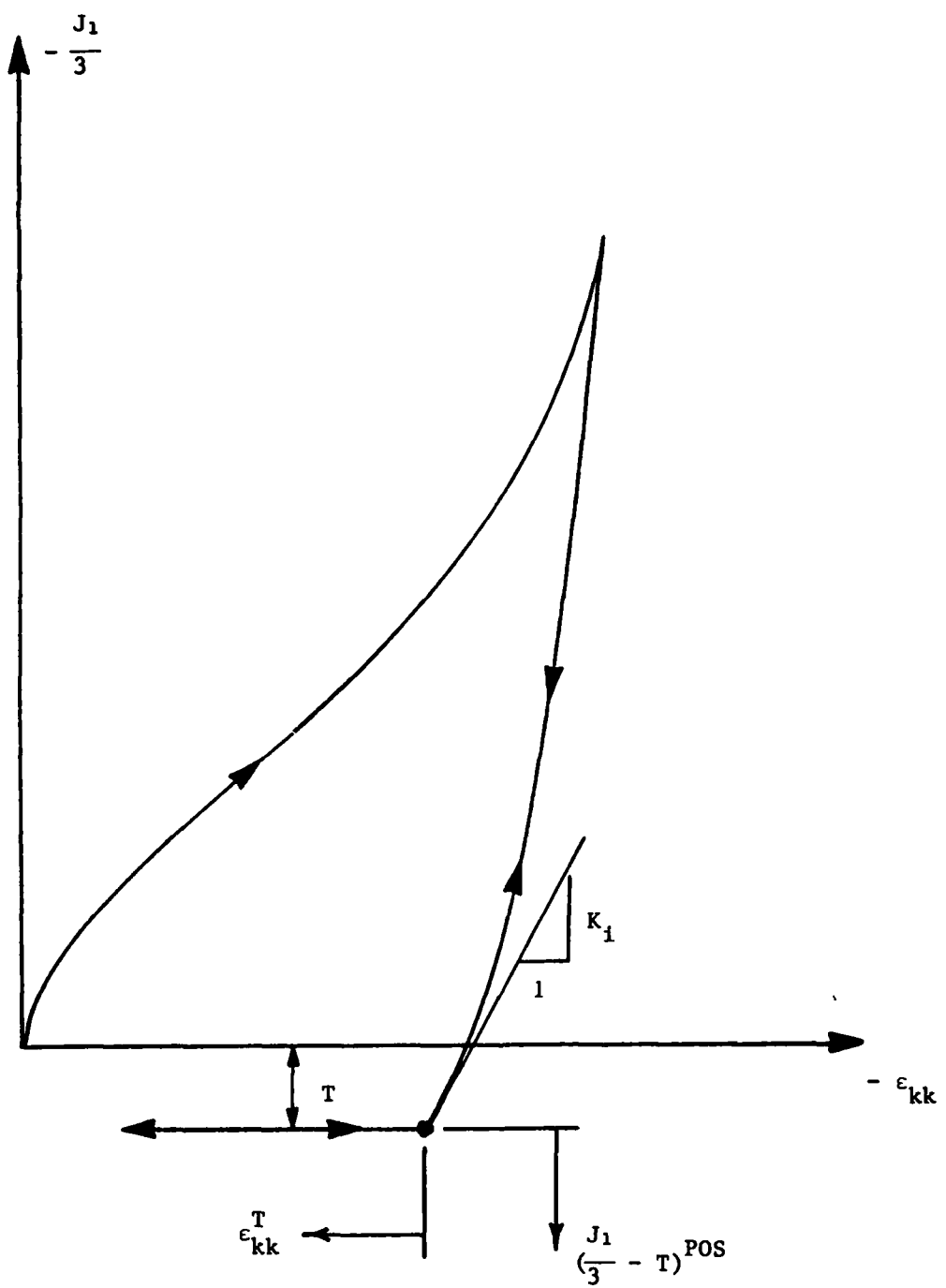


Figure 3. Behavior of the model in tension.

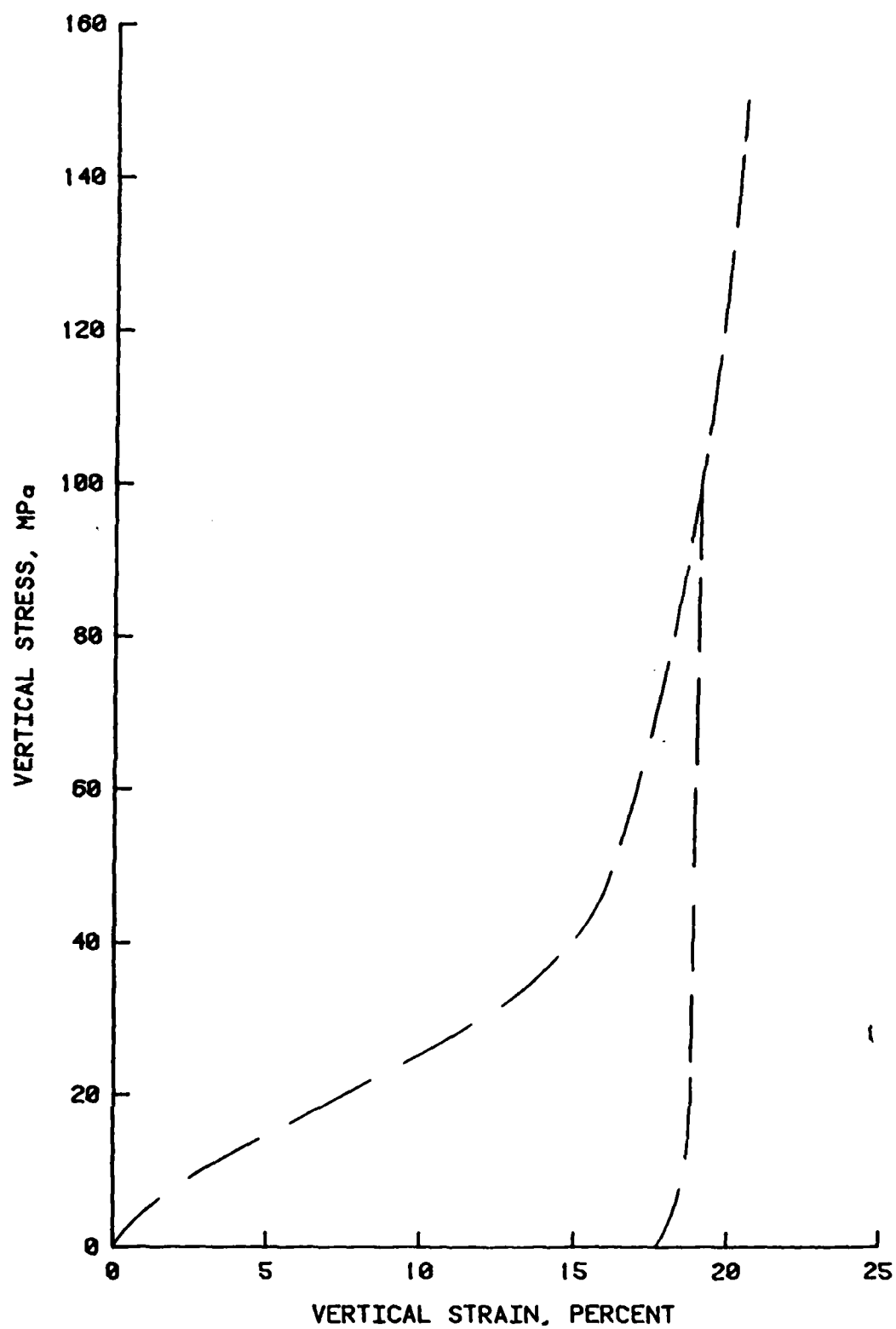


Figure 4. Material properties for ISST Layer 2: uniaxial strain compressibility relation to $\sigma_z = 150$ MPa.

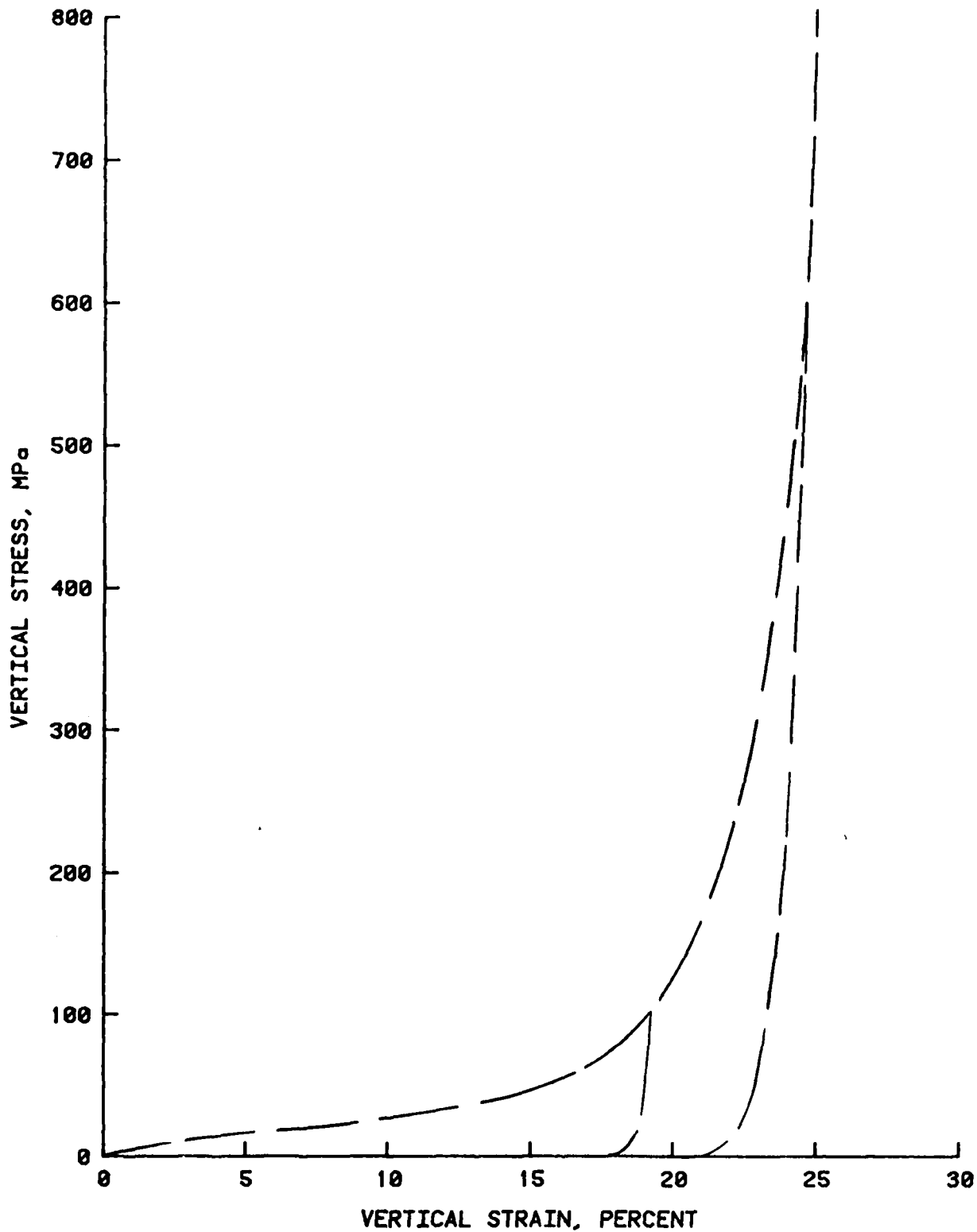


Figure 5. Material properties for ISST Layer 2: uniaxial strain compressibility relation to $\sigma_z = 800$ MPa.

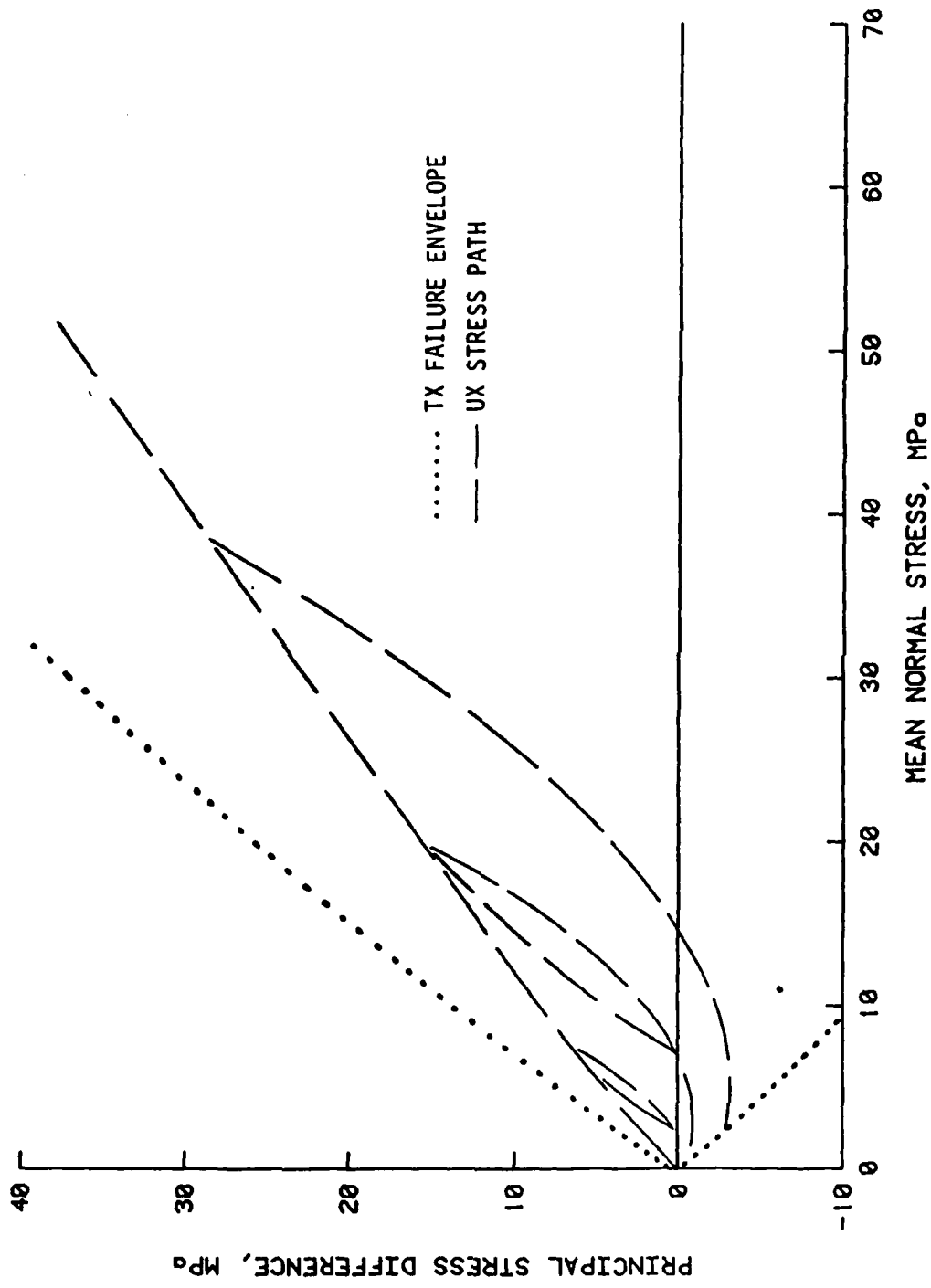


Figure 6. Material properties for ISST Layer 2: UX stress path to $\sigma_2 = 75$ MPa and TX failure envelope.

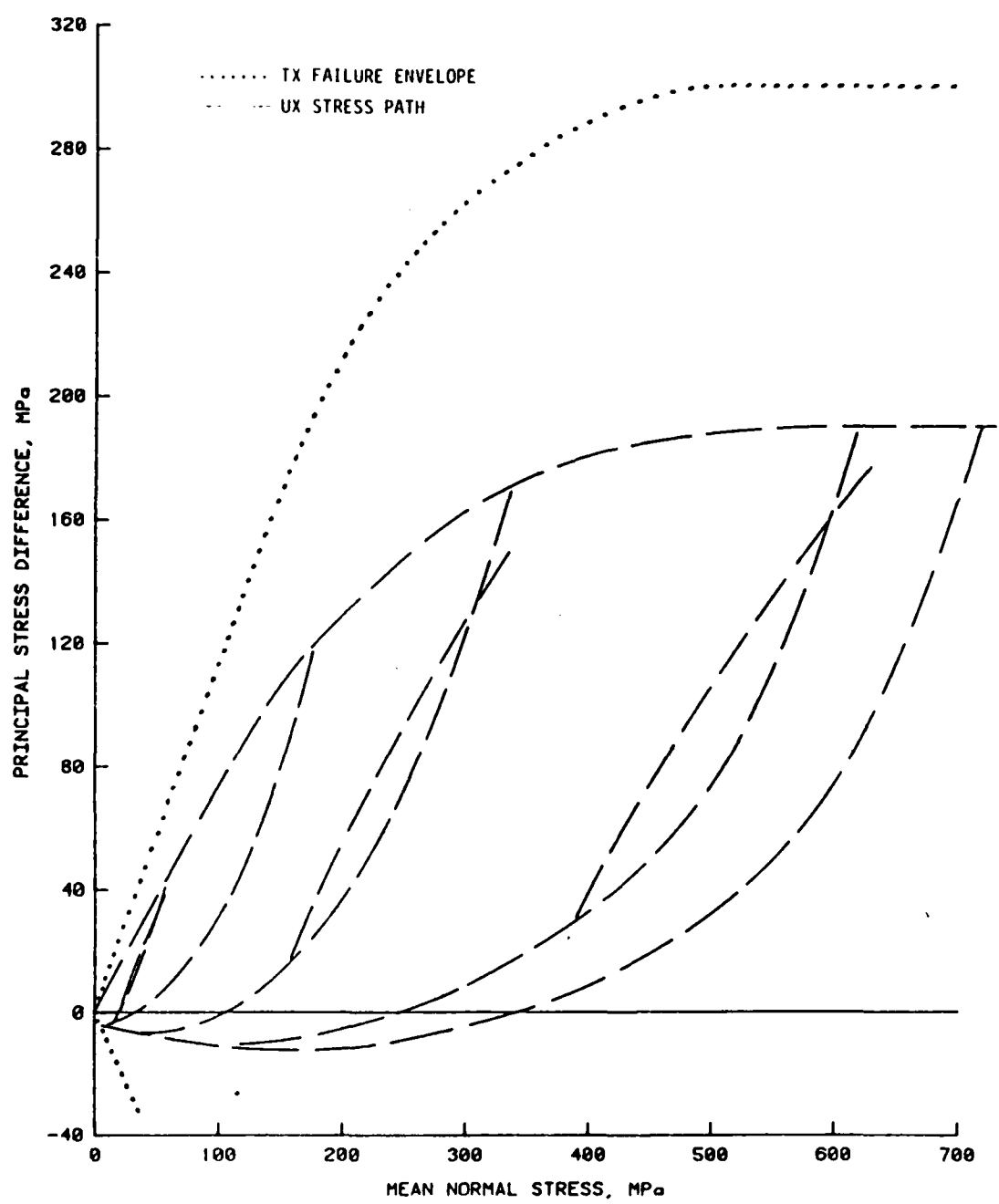


Figure 7. Material properties for ISST Layer 2: UX stress path to $\sigma_z = 800$ MPa and TX failure envelope.

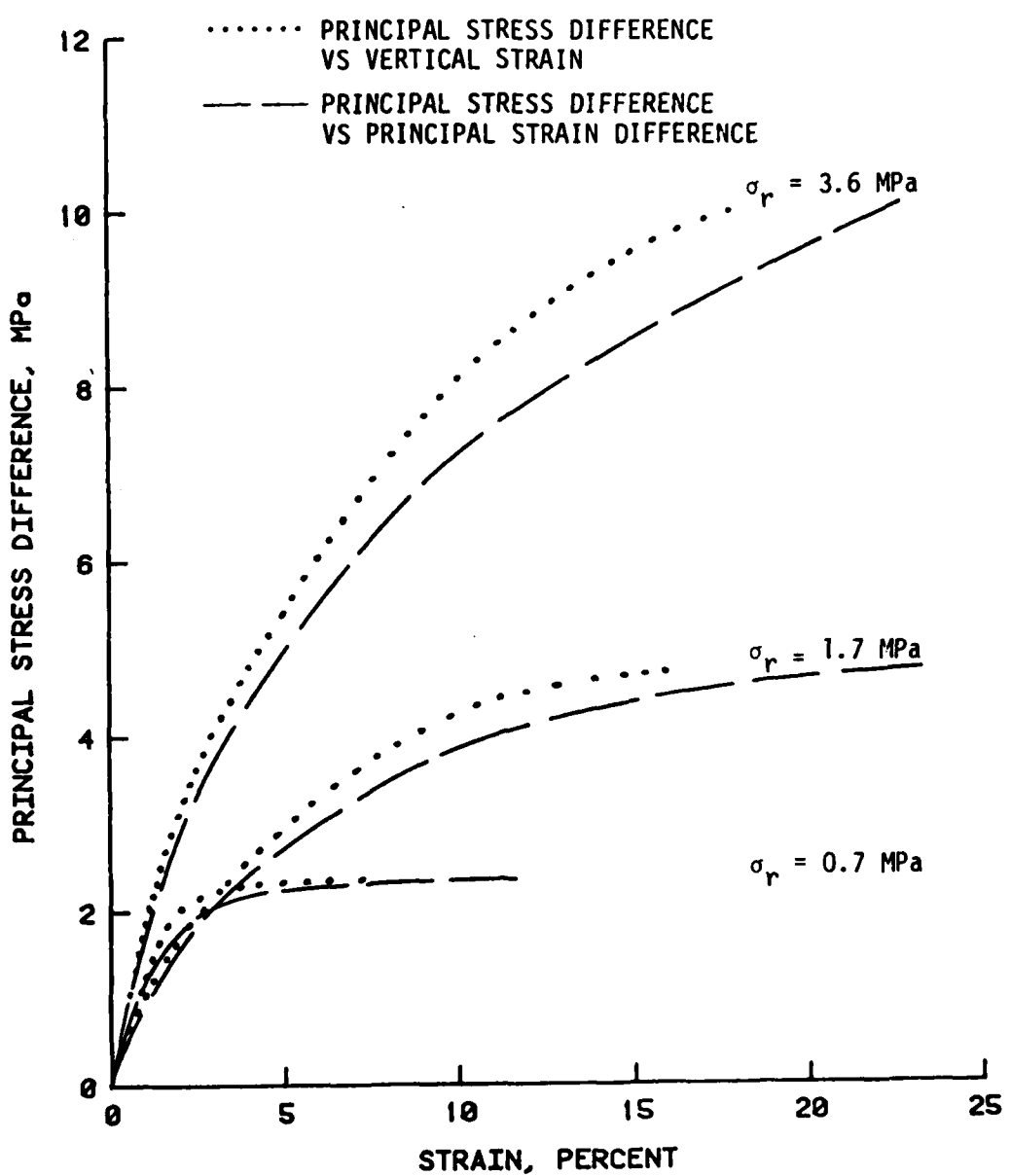


Figure 8. Material properties for ISST Layer 2: triaxial compression stress-strain relations for low confining pressures.

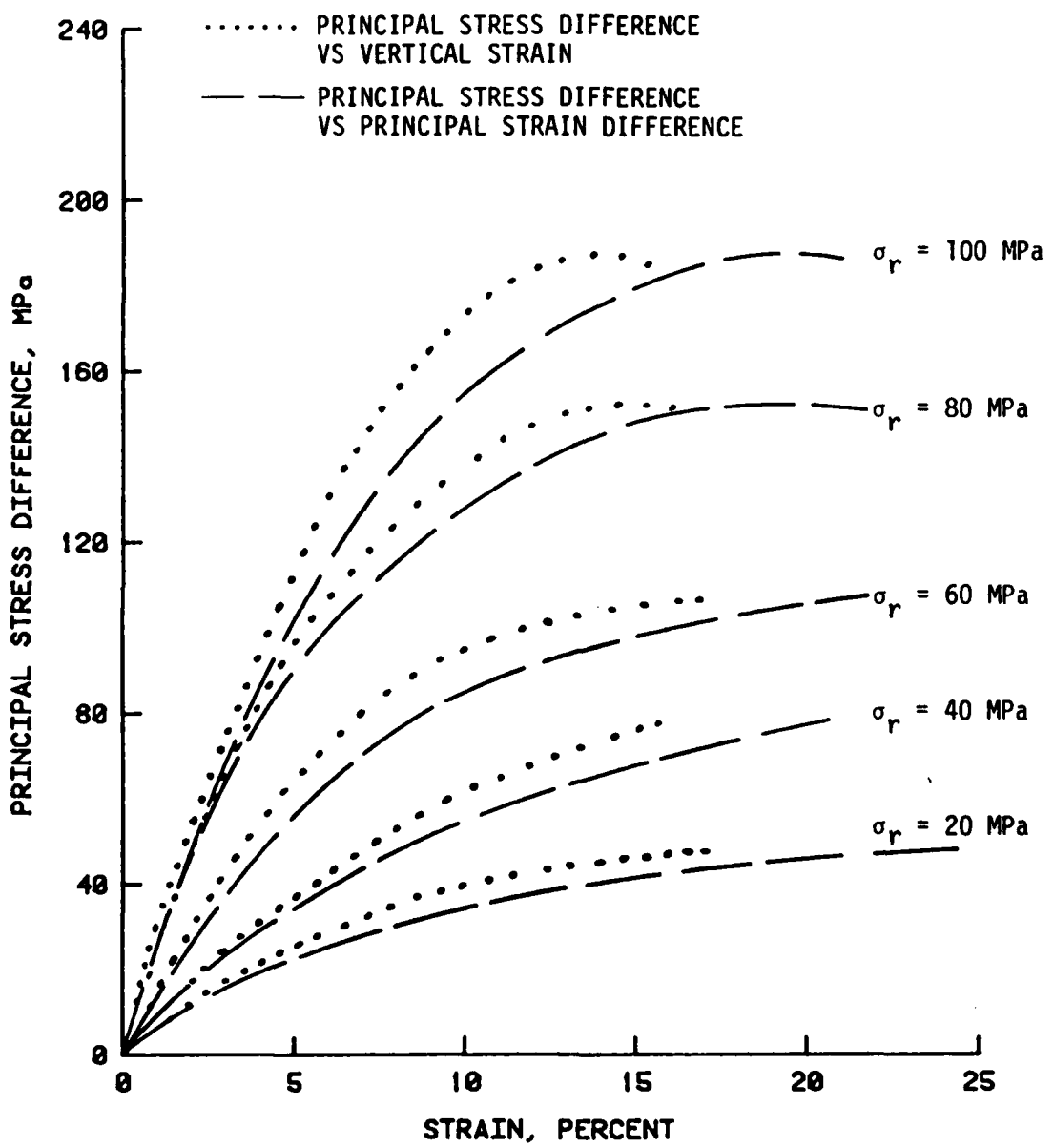


Figure 9. Material properties for ISST Layer 2: triaxial compression stress-strain relations for intermediate confining pressures.

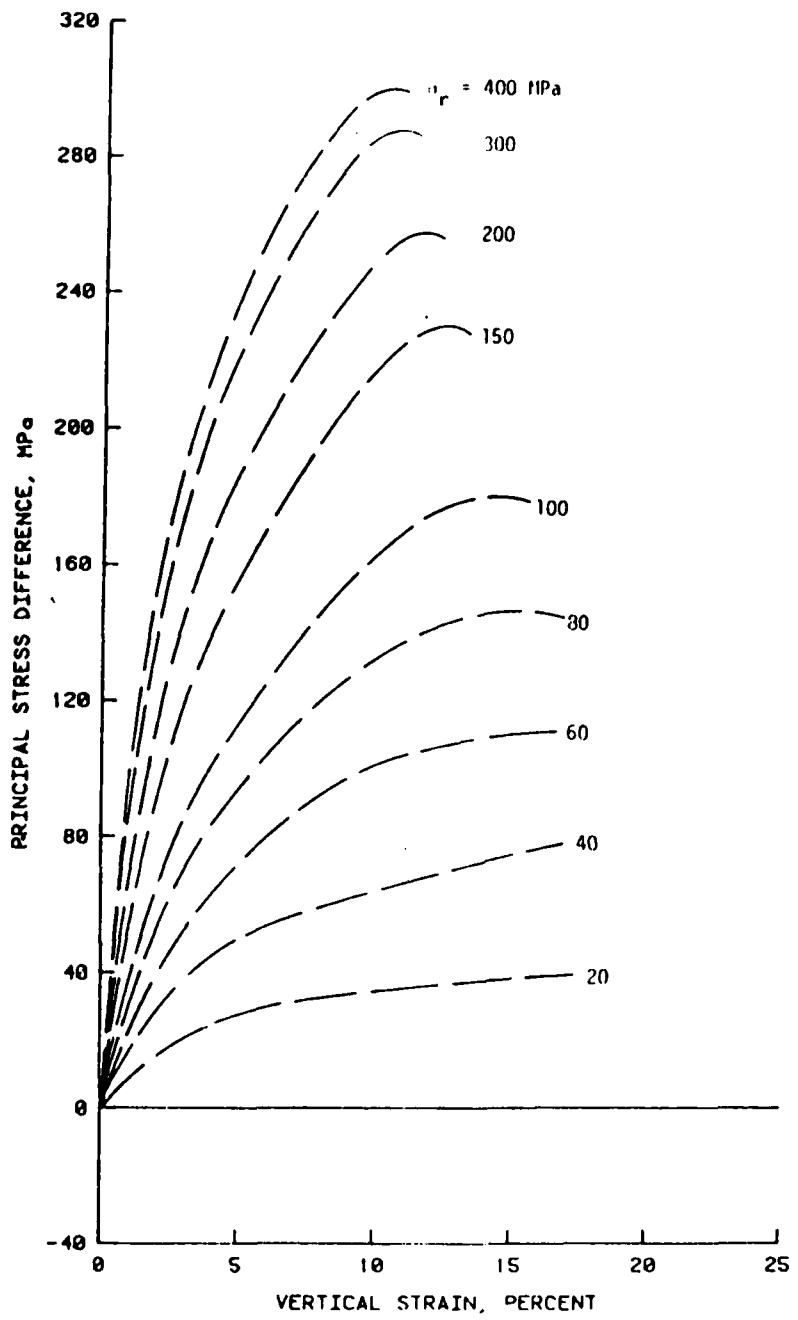


Figure 10. Material properties for ISST Layer 2: triaxial compression stress-strain relations for high confining pressures.

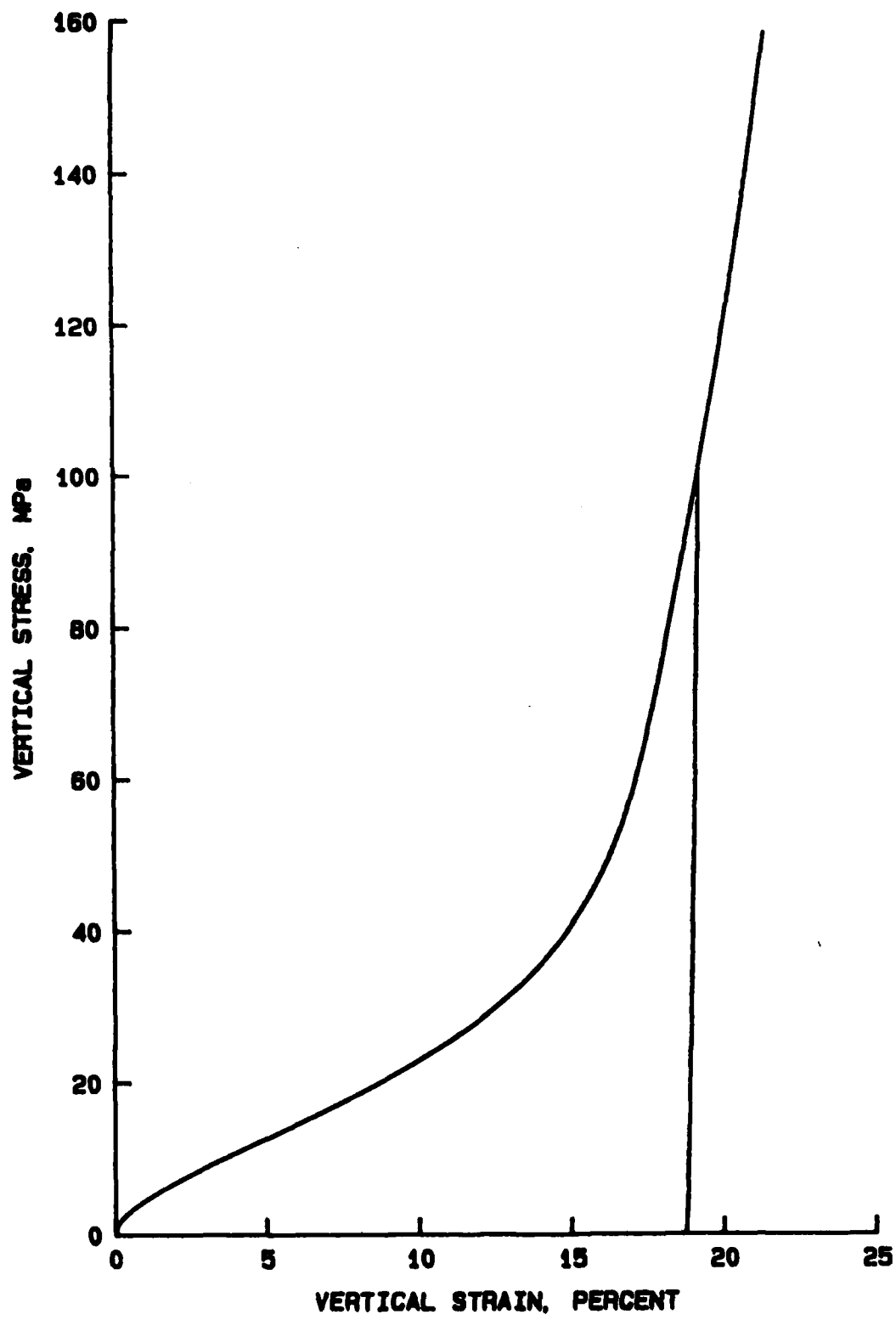


Figure 11. Strain-dependent cap model fit for ISST Layer 2:
uniaxial strain compressibility relation to
 $\sigma_z = 155 \text{ MPa}$.

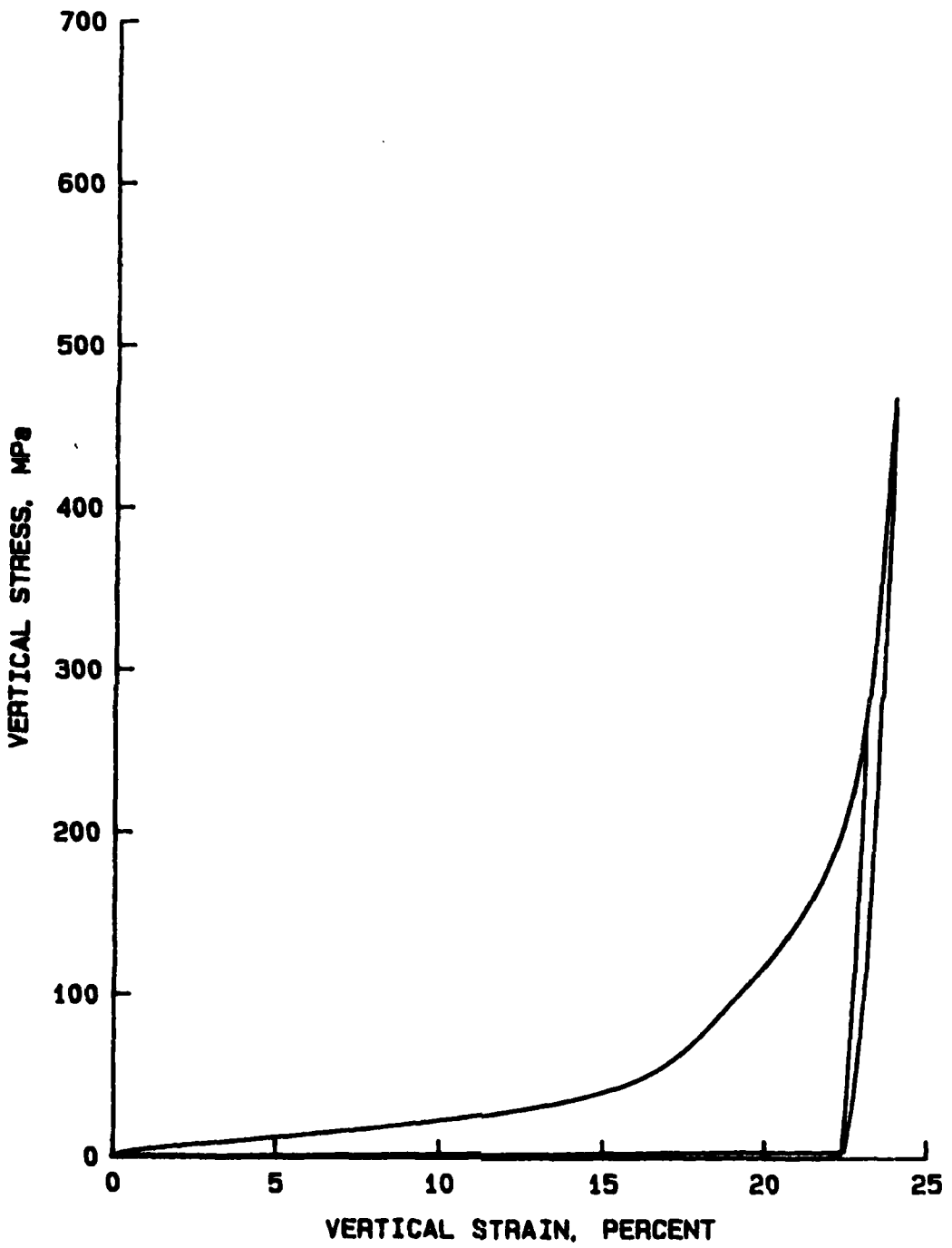


Figure 12. Strain-dependent cap model fit for ISST Layer 2:
uniaxial strain compressibility relation to
 $\sigma_z = 470$ MPa.

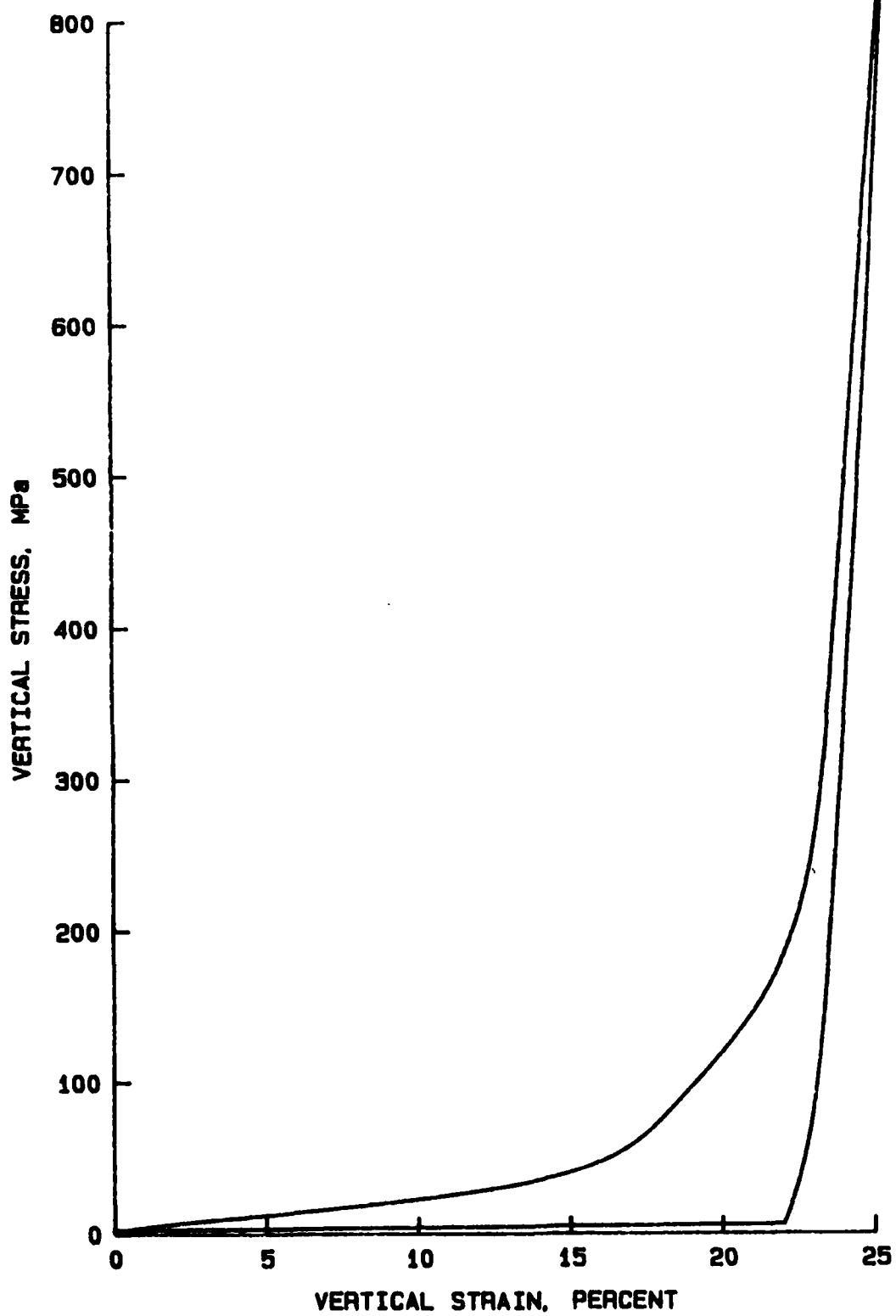


Figure 13. Strain-dependent cap model fit for ISST Layer 2:
uniaxial strain compressibility relation to
 $\sigma_z = 860$ MPa.

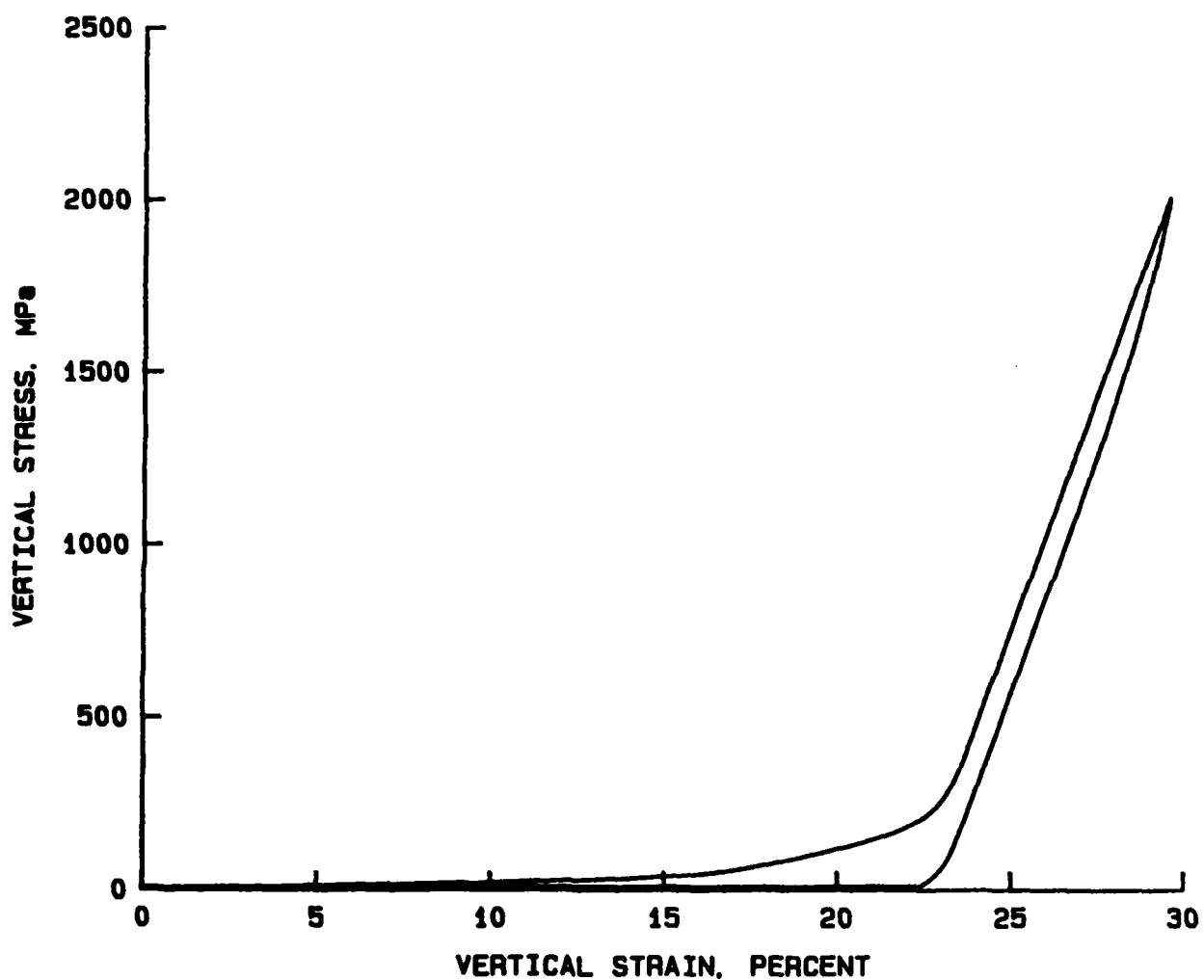


Figure 14. Strain-dependent cap model fit for ISST Layer 2:
uniaxial strain compressibility relation to
 $\sigma_z = 2,000 \text{ MPa}$.

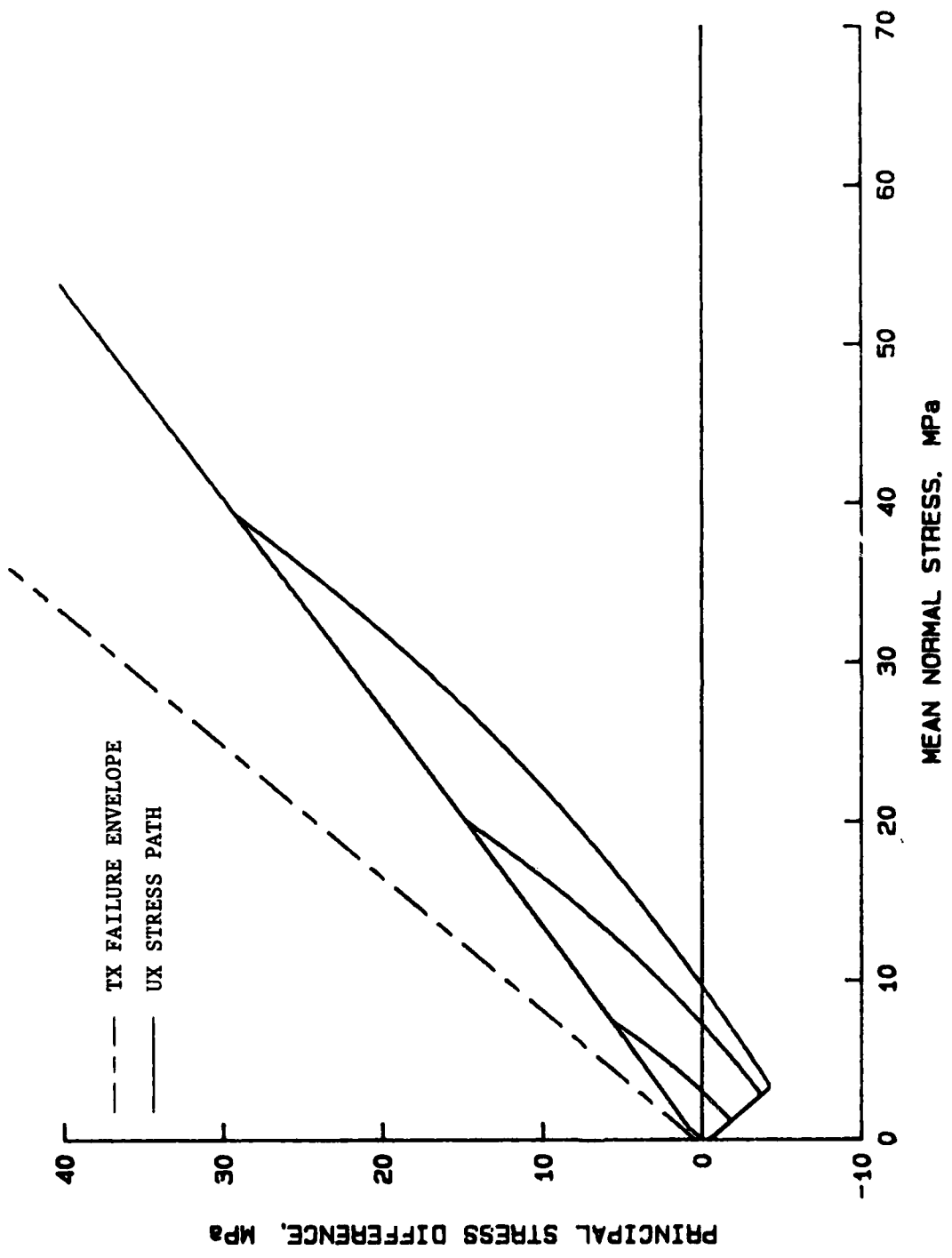


Figure 15. Strain-dependent cap model fit for ISST Layer 2: UX stress path to $\sigma_z = 80$ MPa and TX failure envelope.

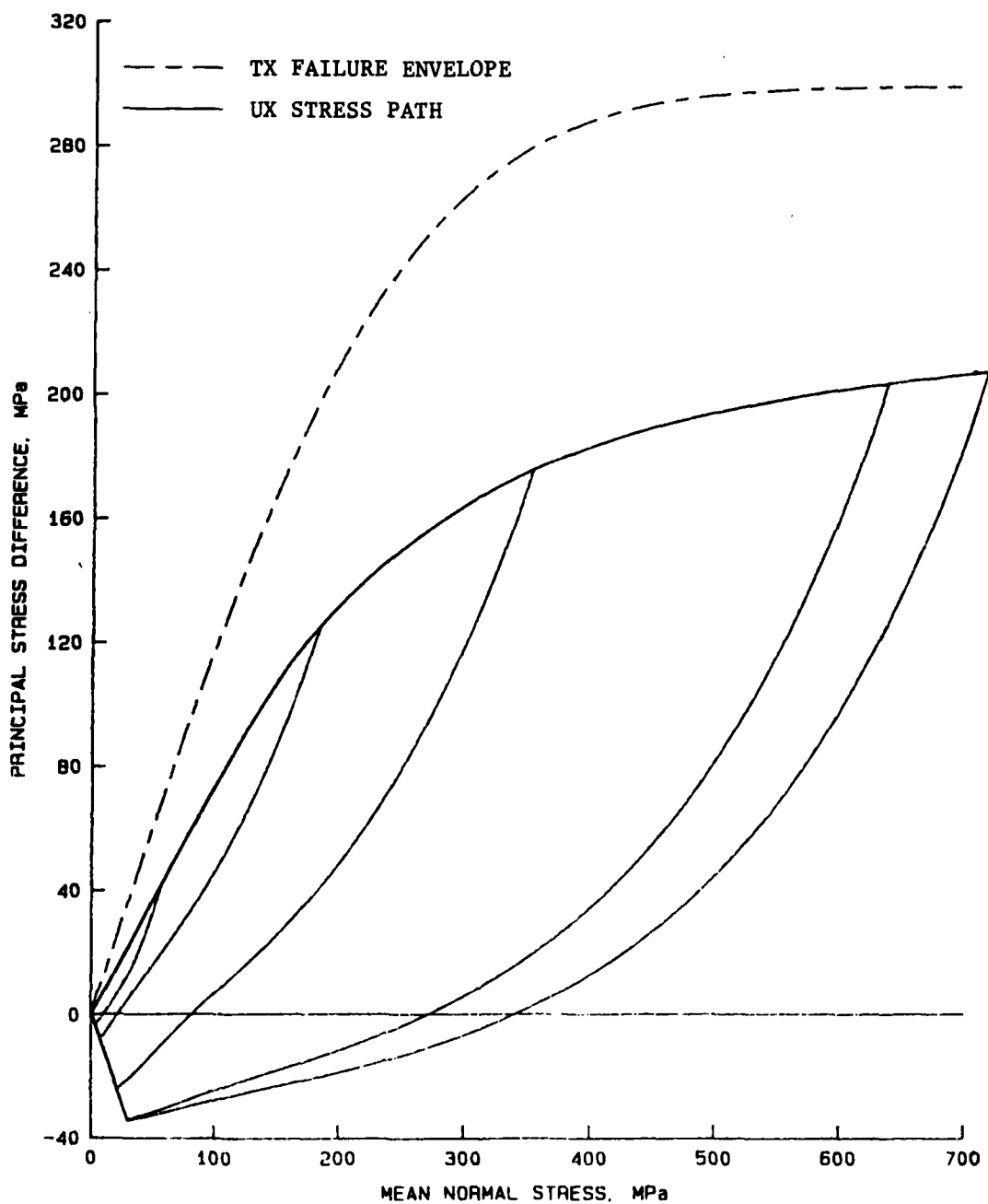


Figure 16. Strain-dependent cap model fit for ISST Layer 2:
UX stress path to $\sigma_z = 860$ MPa and TX failure.

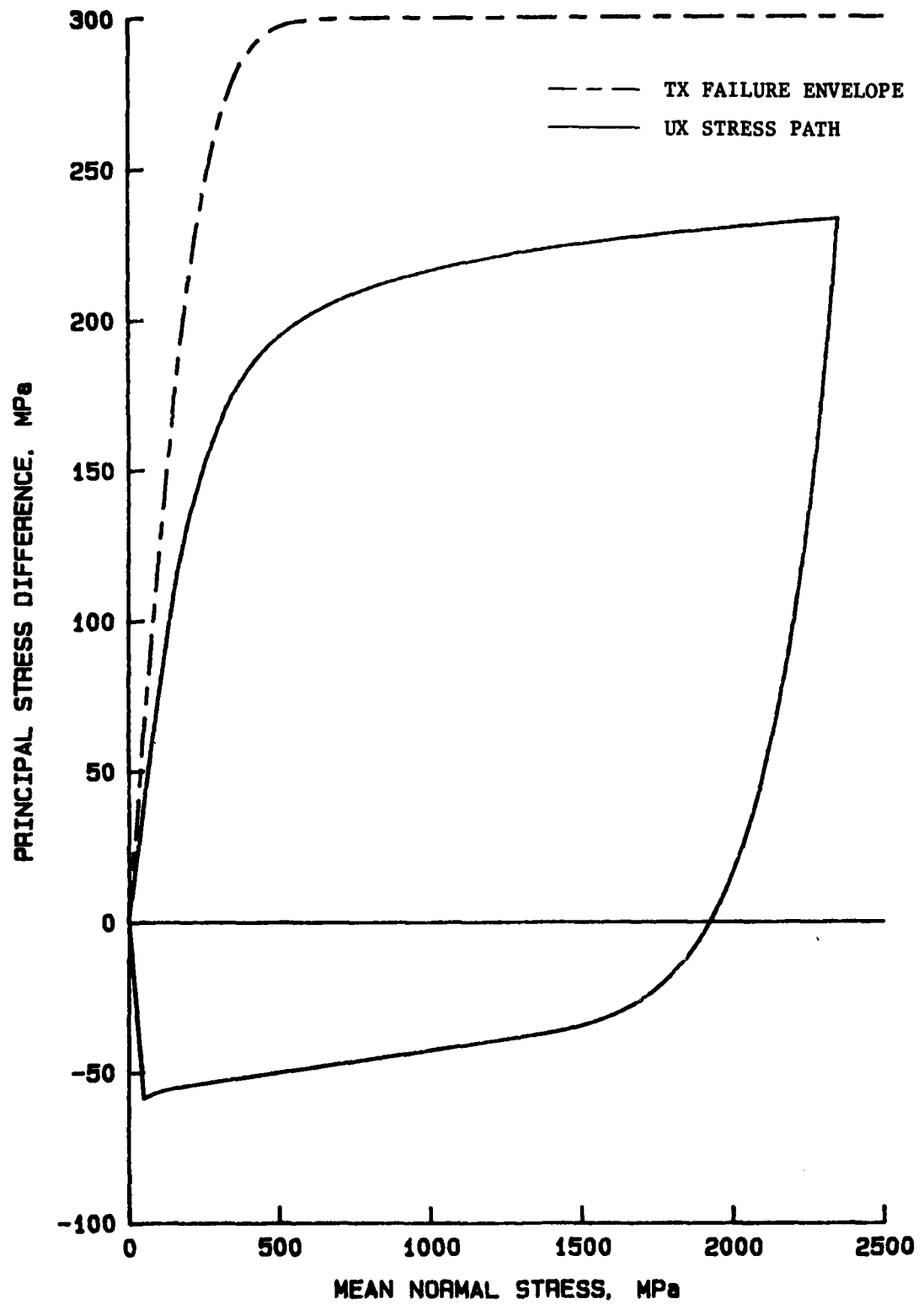


Figure 17. Strain-dependent cap model fit for ISST Layer 2:
UX stress path to $\sigma_z = 2,500$ MPa and TX failure envelope.

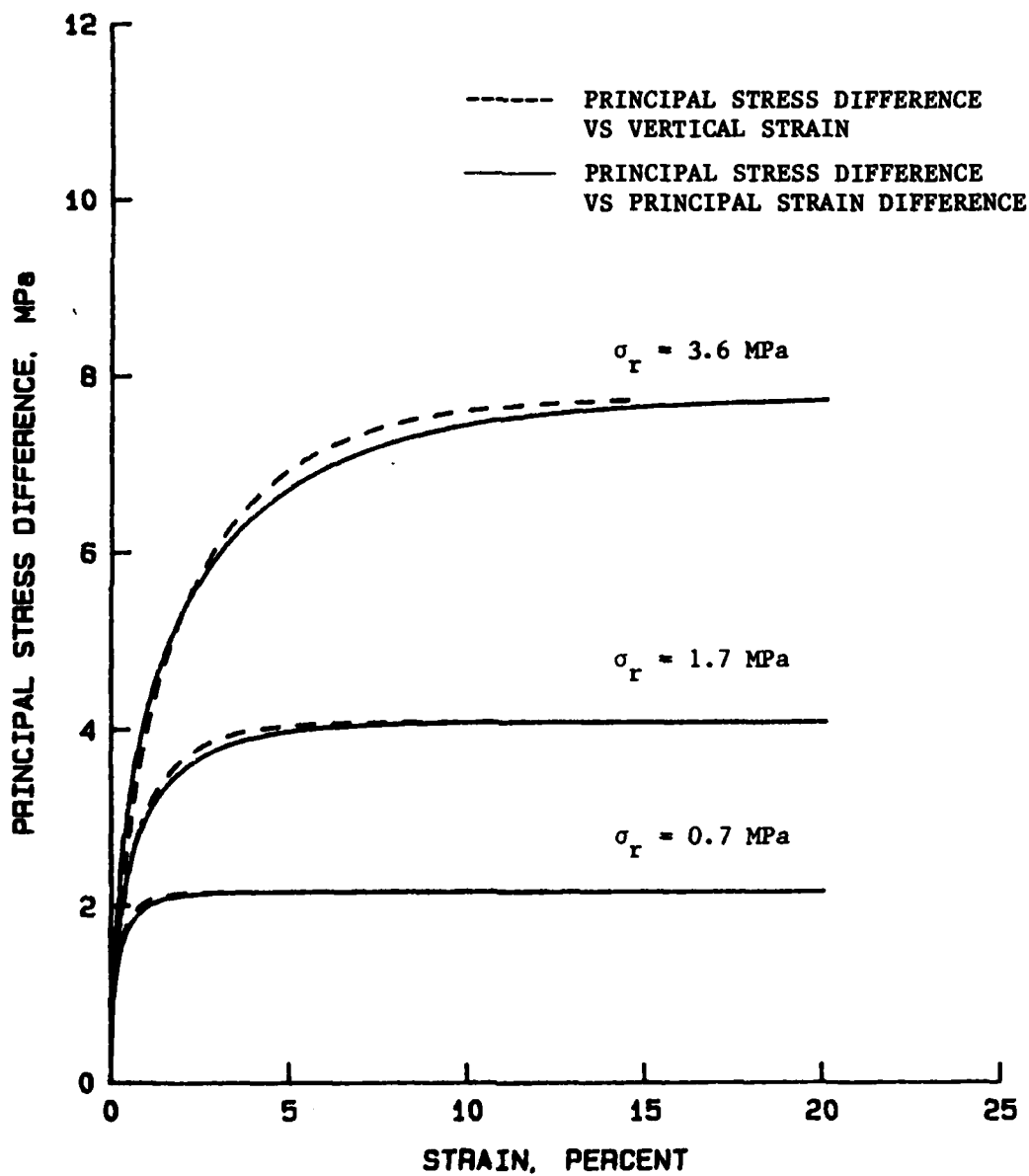


Figure 18. Strain-dependent cap model fit for ISST Layer 2: triaxial compression stress-strain relations for low confining pressures.

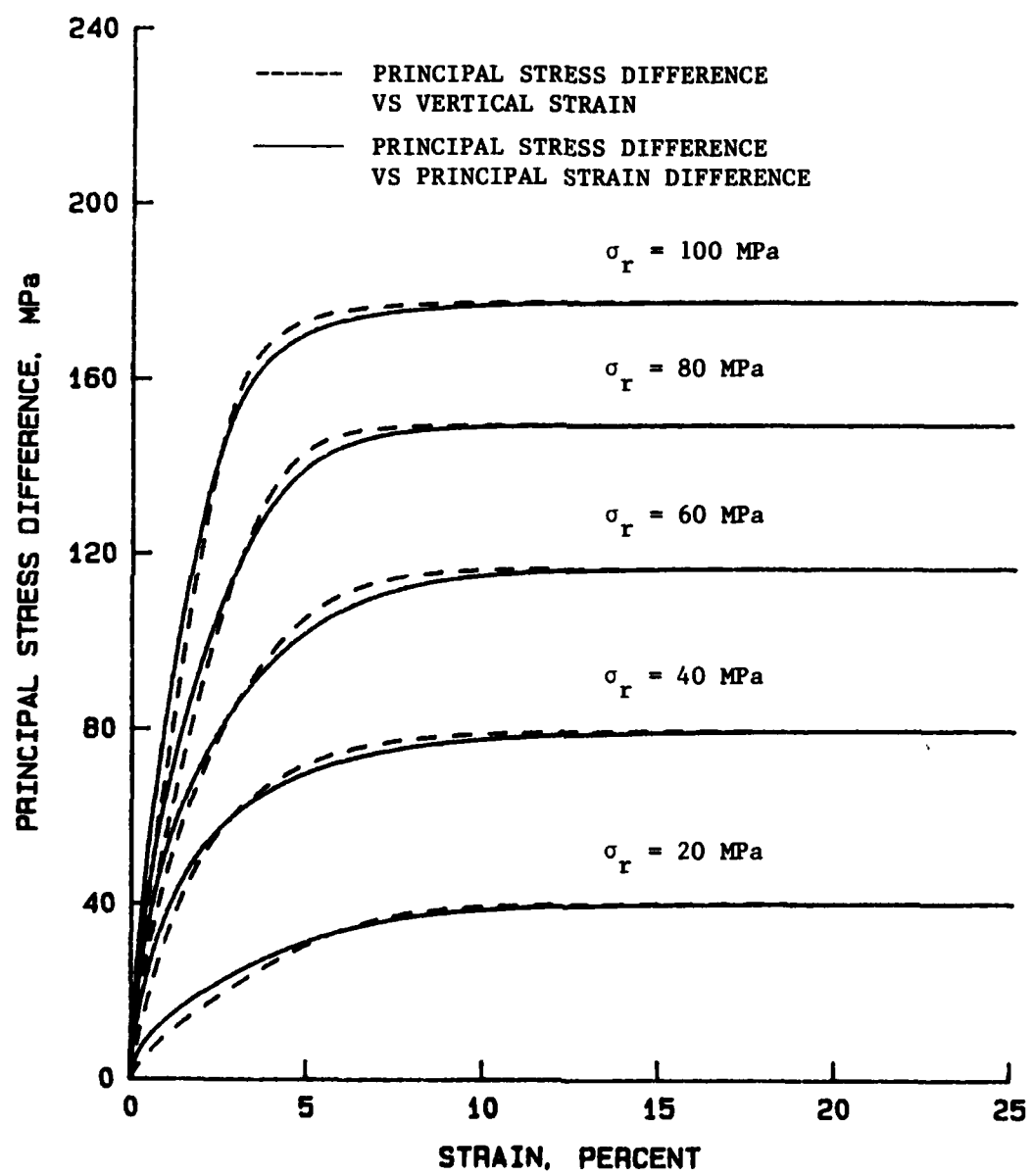


Figure 19. Strain-dependent cap model fit for ISST Layer 2: triaxial compression stress-strain relations for high confining pressures.

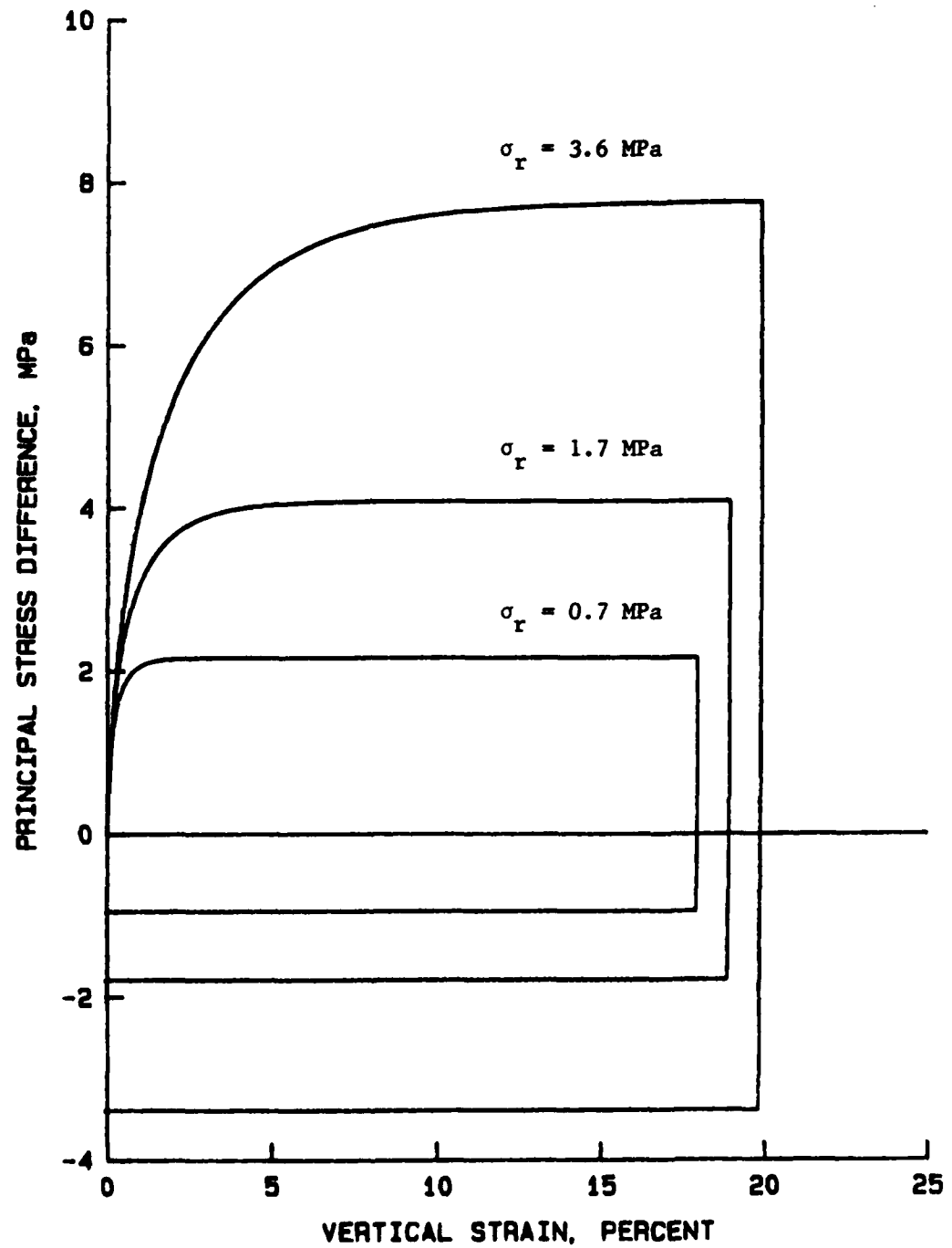


Figure 20. Strain-dependent cap model fit for ISST Layer 2: triaxial compression principal stress difference - vertical strain relations for low confining pressures.

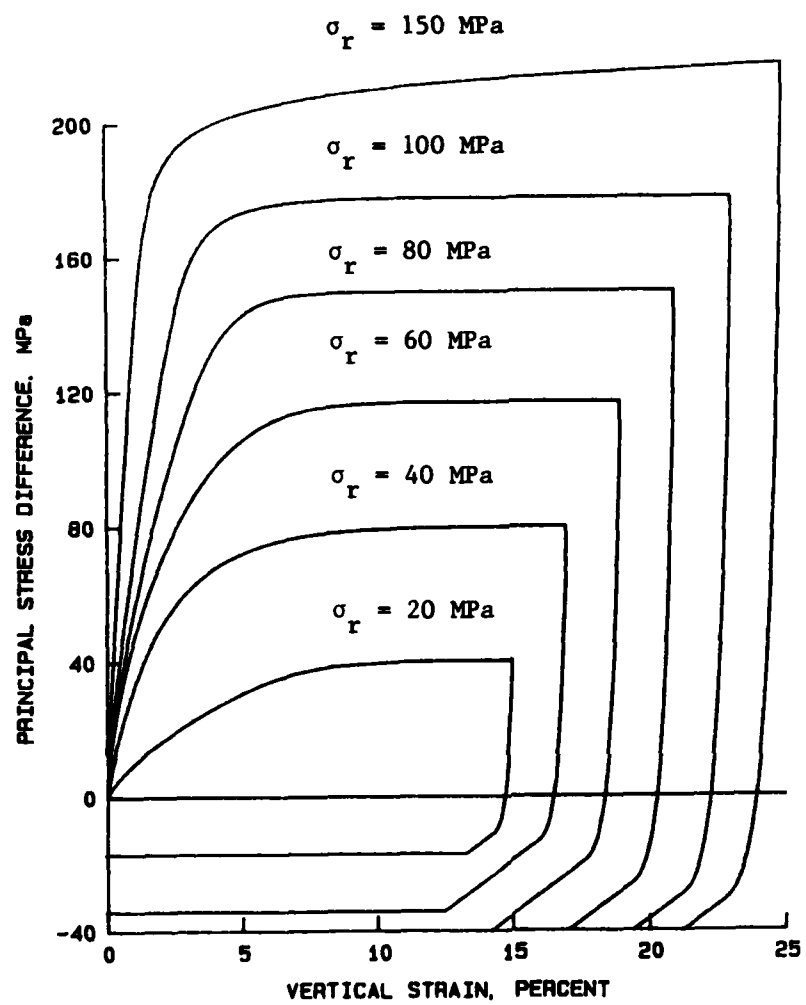
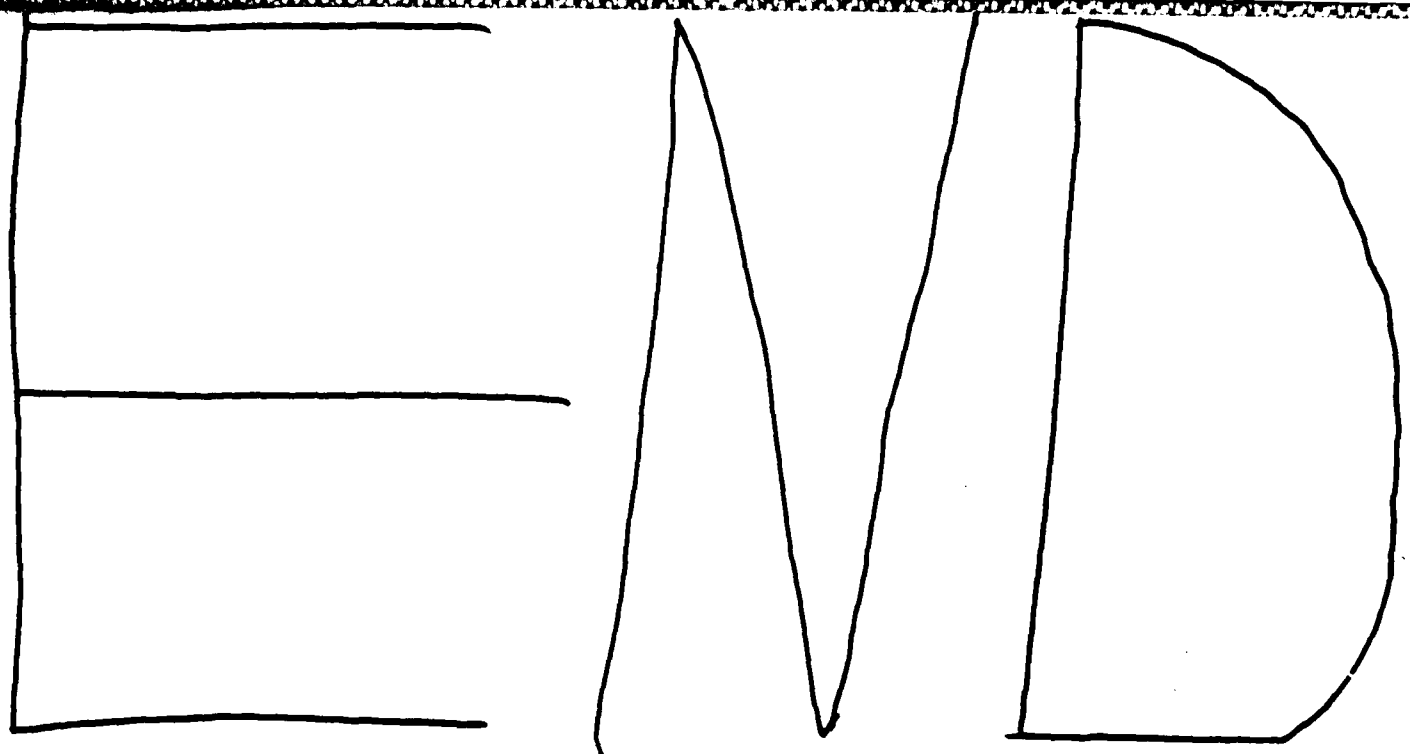


Figure 21. Strain-dependent cap model fit for ISST Layer 2: triaxial compression principal stress difference - vertical strain relations for high confining pressures.

REFERENCES

1. I. S. Sandler, F. L. DiMaggio and G. Y. Baladi; "Generalized Cap Model for Geological Materials"; July 1976; Journal of the Geotechnical Engineering Division, ASCE, Vol. 102, No. GT7, Proc. Paper 12243, pp. 683-699.
2. A. E. Jackson, Jr.; "Preliminary Material Property Estimates for ISST Ground Shock Calculations"; January 1984, U.S. Army Engineer Waterways Experiment Station, Vicksburg, MS.
3. G. Y. Baladi; "Constitutive Model Equations and Parameter Values Used for Fitting Preliminary Material Property Estimates for ISST"; April 1984; U.S. Army Engineer Waterways Experiment Station, Vicksburg, MS.
4. I. S. Sandler; "Material Models for Ground Shock Calculations"; 11 July 1984; DNA meeting on Constitutive Models for Ground Calculations at SRI International, Menlo Park, CA.
5. D. C. Drucker; "On Uniqueness in the Theory of Plasticity"; Quarterly of Applied Mathematics, Vol. 14; 1956.
6. Ivan S. Sandler, Weidlinger Associates, Consulting Engineers; Letter to Dr. J. G. Jackson, Jr., WESSD, submitted to complete Purchase Order No. DACA39-86-M-0057; November 1985.



12 - 86

